Dry Metal Forming Open Access Journal

Final Project Report

Edited by Frank Vollertsen
Available online at https://elib.suub.uni-bremen.de

www.drymetalforming.de

Dry Met. Forming OAJ FPR 6 (2020) 166–191
Date of Report 31 May 2020; published 12 June 2020

Lubricant-free tribology concepts for cold extrusion by interaction-reduced surfaces

(DFG Grant No. HI 790/45; SCHN 735/26; PO 591/37, Funding Period 01.01.2014 – 31.05.2020)

Marco Teller*[1], Stephan Prünte[2], Ingo Ross[3], Moritz Küpper[4], Reinhart Poprawe[3,4], Constantin Häfner[3,4], Jochen M. Schneider[2], Gerhard Hirt[1]

[1]Institute of Metal Forming (IBF), RWTH Aachen University, Intzestr. 10, 52072 Aachen, Germany
[2]Materials Chemistry (MCh), RWTH Aachen University, Kopernikusstr. 10, 52074 Aachen, Germany
[3]Fraunhofer Institute for Laser Technology (ILT), Steinbachstr. 15, 52074 Aachen, Germany
[4]Chair for Laser Technology (LLT), RWTH Aachen University, Steinbachstr. 15, 52074 Aachen, Germany

Summary

The currently most effective approach for reduction of friction and wear in cold forging is the application of lubricants. Scope of the present study is the design and realization of a surface modification concept for forming tools to enable the cold extrusion of aluminum in absence of lubricants. By quantum-mechanical guided design of wear resisting layers with reduced interaction, minimization of adhesion as the main wear mechanism is aspired. Through smoothing of roughness peaks and topography homogenization the laser assisted surface modification of the tools systematically aims at minimization of abrasive wear and thus less wear particles that act as nuclei for adhesive processes. Evaluation of the developed structures and layers is carried out on a newly designed torsion-tribometer, which enables the free scaling of contact stress and slide path combined with a certain amount of surface expansion. The report first gives an insight into the current state of the art, analyses the load case during cold extrusion and derives suitable tribological experiments for the characterization of adequate surface modifications. Subsequently, laser polishing and structuring processes are presented and, based on a quantum mechanical calculation of the interaction between tool and workpiece (aluminum), a possible solution concept by the use of self-assembling monolayers is presented. Finally, the methods are combined and their influence on adhesive wear is highlighted in tribological tests.

Keywords: Extrusion, cold forging, tribology, tribological testing, aluminum, self-assembling monolayer (SAM), laser polishing, laser structuring

1 State of the art

1.1 Tribology in industrial cold extrusion

According to DIN 8582, impact extrusion belongs to the group of compressive forming processes. Its special advantages are, among other things, the optimal use of material, the low unit costs as well as the reproducible high dimensional accuracy and surface quality of the workpieces. Increased strength due to work hardening and a stress appropriate fibre orientation is a favorable prerequisite for an increase in economic importance [1]. The challenges on the process side consist primarily in the interpretation and control of the tribological effects between tool and workpiece with regard to possible tool damage as well as in ensuring the required surface quality of the workpiece. In contrast to the tribological conditions of other technological processes a

*E-mail address of corresponding author: marco.teller@ibf.rwth-aachen.de

very high contact pressure prevails during impact extrusion, which is dependent on the tool geometry and the material flow and can reach a multiple of the initial yield stress of the workpiece. In cold extrusion, surface pressures in the range of 4 to 9 times of the initial yield stress of the workpiece are quite common [1]. In individual cases contact pressures of up to 4,000 MPa can be achieved [2].

In connection with the strong surface enlargement (by 2 to 11 times) of the workpiece the high contact pressures can quickly lead to severe wear on the tools. This manifests itself in inadmissible changes in shape and dimension of the surface of the tool and the workpiece [3] and is clearly the most frequent cause of failure for tools in forming technology. Tool wear and the associated repair costs and maintenance are therefore of central economic importance for process control [4].

According to current understanding, the physical and chemical processes occurring during wear are based on the four wear mechanisms abrasion, adhesion, tribochemical reaction and surface disruption [5,6]. The relevant mechanisms in the practice of cold forging are abrasion and adhesion [1]. Abrasive wear is caused by surfaces with hard protruding particles that slide against another surface. Hereby chips or small particles are produced, which are deposited e.g. in scratches on the softer surface. This is usually an unavoidable long-term effect.

The adhesion mechanism is of particular importance for cold extrusion [7]. In this case, micro-welding occurs initially at the roughness peaks. Phenomena such as work hardening at the contact of the roughness peaks or diffusion can lead to the adhesive bonds having a higher strength than the base material. In this case, the fracture path would run through the base material with the lower strength [5]. After this initial damage, the adhered wear particles would now plough through the softer material and cause lasting damage to the surface. This generally results in a rapid increase in adhesion, since locally excessive surface pressures arise at these points and chemically identical friction partners with a high tendency to adhere interact. The most important factor influencing the occurrence of adhesive wear is the adhesion tendency of the base material, which is particularly pronounced in the forming of stainless steel or aluminum. The influence of the temperature prevailing in the forming zone has also been demonstrated [8].

The most effective protection against tool wear in cold forging is the use of lubricants [9-11]. The most important task of lubrication is to separate the workpiece and the tool surface from each other, which effectively prevents adhesion in particular and thus reduces tool wear as well as ensuring consistent quality of the pressed parts and undisturbed production. Lubrication is also intended to reduce friction losses. The choice of lubrication can also depend on other criteria, such as: The coupling of lubricating and cooling effects; the influence on the flow of material during forming; the influence on the surface quality of the pressed part; the difficulty of forming; the ability to apply and remove the lubricant; the corrosion protection effect; compatibility with subsequent machining processes and cost-effectiveness [1].

The control of the sophisticated tribological system in industrial cold extrusion is currently mainly achieved by the use of organic and inorganic lubricants. In addition to the lubrication properties, there are a number of other factors that must be taken into account when using lubricants. These include price, environmental issues, availability and the effort required to control the application of the lubricant system. After the forming process, the lubricants must be removed from the product and disposed of properly [12].

Therefore, there are still numerous efforts to increase the tool life by selecting appropriate materials [13] and by applying surface layers or a corresponding surface layer functionalization, thus qualifying the tribological system for forming without lubricants.

1.2 Surface layers for wear reduction

A major wear mechanism is the adhesion between tool and workpiece (Fig. 1). The underlying wear mechanism is defined as follows in a recent overview [1] by Groche:

"Adhesive wear is based on the formation of chemical bonds at individual contact points between metallic bodies by free cohesive forces [...], which break up again when relative movement occurs in the plane of minimum shear strength. At high adhesive forces the shear plane shifts to the softer friction partner [...]. The strength of the adhesion depends on the number of [...] microcontacts, the size of the bonding forces acting between the partners and the electron configuration of the metallic bodies involved." (translated by the authors from German)

It follows that - regardless of whether a tool protection layer has been applied or not - the shifting of the shear plane out of the original sliding joint into the tool or workpiece must be prevented in order to avoid adhesive

wear. This can be achieved by specifically influencing the chemical interaction between tool surface and workpiece, e.g. by applying a corresponding functional layer.

The commercially available protective coatings for wear reduction in forming technology are often based on material developments for cutting technology. The protective coatings for cutting tools are characterized by very high chemical stability and wear resistance and are often deposited on hard metals. Potential materials for these applications are transition metal nitrides and carbides [14] and transition metal aluminum nitrides [15-17]. The protective layers are deposited in various thicknesses from a few nanometers (thin layers) to the millimeter range (thick layers) by means of various (plasma-assisted) processes (PVD, CVD, deposition welding). According to Clarysse et al. [14], the selection of suitable protective coatings for forming processes has so far mostly been carried out using the trial-and-error method. It was shown that the use of hard and brittle coatings on tool materials that are relatively soft compared to cutting tools reduced the performance. For this reason, measures are being taken to increase the load-bearing capacity of the tool surface layers, e.g. (plasma) nitriding [14,15], while the alternate deposition of hard material layers and (metallic) layers with lower rigidity enables the formation of "multilayer" structures, which significantly increases the fracture toughness of the layer systems.

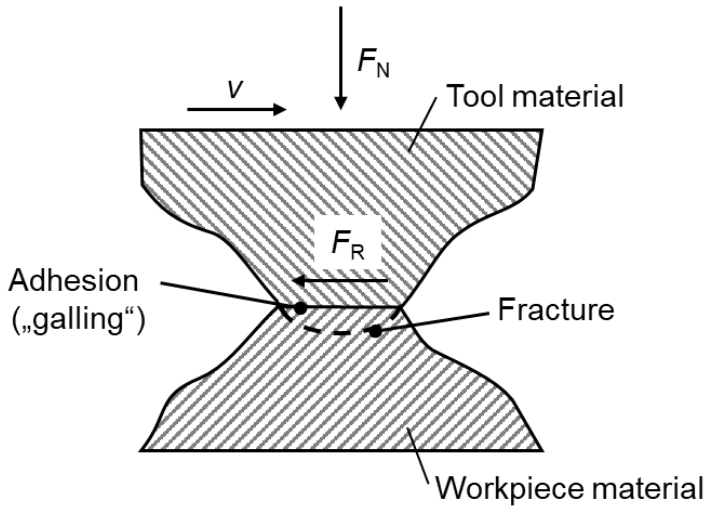

Fig. 1: Occurrence of cold welding in metallic contact. [6]

Little has been reported on the use of these coatings in dry forming; according to the current state of the art, the improvement of resistance to adhesive wear is achieved exclusively by the use of lubricants [1,5]. The above mentioned facts, especially the connection between adhesive wear and the formation of chemical bonds described by Groche in a recent review [1], motivate the research strategy of quantum-mechanically guided design of tool protection layers with minimal chemical interaction between tool and workpiece, which is unconventional for metal forming technology. It is expected that on the basis of this material design approach the adhesion wear will be significantly reduced, thus enabling low-wear dry forming.

1.3 Surface structures for wear reduction

While the cause of abrasion is largely understood, the function of adhesion has not yet been sufficiently clarified [18]. The development of high adhesion forces requires, among other things, the microgeometric adaptation of the paired surfaces as well as macro- and microgeometric surface enlargements of the friction partners, as they occur during forming at micro-contact points of roughness [1].

In the field of surface modification, (mechanical) polishing is widely used to remove defects and rough structures protruding from the surface, which can serve as starting points for an adhesive material transfer from the workpiece to the tool. For wear tests on laboratory scale, tool surfaces are therefore polished to a roughness of $Ra < 0.1$ µm. For industrial applications, however, these roughnesses are sometimes very difficult to achieve, partly due to limited accessibility. Therefore, large, complex tools are usually at least partially polished manually and minimum roughnesses of $Ra = 0.2$ µm are achieved. [19].

Overall, the surface topography has a decisive influence on the tribological conditions in the tool and workpiece surface system [20]. The use of a functionally adapted surface design to improve the tribological properties in forming processes is therefore an essential part of current research and development [21]. Mechanical

(SBT: Shot Blast Texturing), electrolytic (EDT: Electro Discharge Texturing, EBT: Electron Beam Texturing) as well as laser-assisted (LT: Laser Texturing) structuring processes are used, for example, to help steel strip achieve more favorable deep-drawing properties by means of defined structural features during cold rolling [22].

Previous studies on laser structuring of forming tools have been exclusively investigated for tools that use lubricants during the forming process at the same time. In addition, Wagner et. al. [23] show that the life time of the forming tool can be increased by selective surface treatment of the forming tool with laser radiation. Characteristic material properties such as hardness, residual stress, retained austenite content, etc. are specifically adjusted by laser treatment.

As these results only refer to forming processes using a lubricant, their transferability to lubricant-free forming processes is only partially given. A significant difference can be expected for the dimensions of structures, since lubricants have a significantly different flow behavior than the material to be formed. In particular, sub microscale structures will most likely not have a significant influence on the wear behavior.

The interaction between different surface roughnesses, structures and materials and their influence on the coefficient of friction in forming tools without the use of lubricants has not been described sufficiently so far. Experimentally as well as analytically and numerically this analysis is a challenge.

So far, no investigations have been carried out on the interaction between surface topography, characteristic material properties and tool surface in the field of lubricant-free forming. The interactions are therefore only insufficiently known or described. Since surface topography [14] or roughness [19] and microstructure [24] have a significant influence on abrasive and adhesive wear, a systematic investigation of these influence-effect relationships is necessary.

1.4 Tribology characterization in forming technology

The determination and description of the tribological conditions is still theoretically only possible to a very limited extent due to the manifold phenomena. Therefore experimental investigations play a major role. The good transferability of the results of real tests is contrasted with the high risk of tool damage. Furthermore, the local conditions are hardly analyzable and therefore systematic parameter variations are impossible. The statements obtained usually only refer to the investigated component [25].

Test methods that map areas of a process under conditions that are as homogeneous as possible are widely used. The advantage of these tribometer tests is that they are relatively simple and inexpensive to carry out and the environmental influences on the contact conditions can be easily limited. Different test principles are available for different contact conditions: pin-on-disc, ring-on-disc, etc.

A transfer to forming technology is problematic, since the workpiece is not in the plasticized state. Numerous analogy experiments have therefore been developed in the field of sheet metal forming in order to represent the contact and load conditions in the individual areas of the workpiece during deep drawing as realistically as possible [26]. However, the transferability of the results to bulk metal forming is problematic, since the expected surface enlargement cannot be assumed and the contact pressures that actually occur cannot be achieved in a scalable manner. The Burgdorf ring compression test [27] or the further developed conical tube-upsetting test are still used for this purpose. Well-known methods for the description of local load cases in closed dies are the reduction test, which allows conclusions to be drawn about the respective tribological system by means of relative force comparisons of individual test series [25], and the sliding compression test, which aims to directly determine the friction coefficients under realistic loading [28]. Various test setups have been presented for the tribological characterization of aluminum extrusion [29]. The configuration of a torsion tribometer according to [30] appears promising for the adaptation of the tribological conditions during cold extrusion.

Depending on the forming process under consideration, the tribology characterization depends on the realistic representation of the contact conditions with regard to surface pressure, surface enlargement, relative speeds and sliding path. For bulk deformation the difficulty is that up to now there is no basic experiment where the normal pressure is freely scalable as a multiple of the yield stress and the sliding paths are long enough to analyze the influence of several load cycles.

1.5 Conclusion and goals

The most common and currently most effective method of reducing friction and wear in cold forging is the use of lubricants. The development of coating concepts and functional surfaces has so far been empirically guided and aims at the use of structures as lubricant reservoir. However, it is only possible to completely dispense with lubricants in cold forging if the leading wear mechanism adhesion can be effectively prevented. The quantum-mechanical design of adhesion-minimized surface layers in combination with the functionalization of the surface layer by adjusting the micro-topography in a targeted manner provides a starting point for this.

Following the development towards dry machining in machining technology, the aim of this investigation is to optimize the tribology of cold extrusion by using modified surfaces (structures) and the quantum-mechanically guided design of adhesion-minimized surfaces in order to enable lubricant-free processes in cold massive forming. The goals in detail:

- Development and synthesis of adhesion-minimized layers by quantum-mechanically guided design of protective layers,
- Development and implementation of modified surfaces (structures) to minimize wear and friction
- Development of a tribological test sequence for the characterization of friction and wear properties during cold extrusion of aluminum,
- Evaluation of layer systems and surfaces in tribological tests taking into account contact stresses and sliding paths in the real process and
- Development of a tool concept with locally adapted surfaces for dry forming during cold extrusion of aluminum.

2 Process analysis and development of a tribological test sequence

2.1 Process analysis

For the selection and design of suitable analogy tests, knowledge of the prevailing load spectrum is necessary first. As already explained in the state of the art, different process variables have an influence on friction and wear. In metal forming technology these are generally:

- Local plastic strain
- Relative contact stress (Relative contact pressure)
- Relative velocity between tool and workpiece
- Temperature

The influencing factors listed are not independent of each other. In cold forming, a higher local deformation inevitably leads to a hardening of the material and thus to higher normal stresses. The workpiece temperature is also increased by dissipation and friction, which can cause the flow stress to decrease locally. In addition, the load spectrum in full forward extrusion depends on the tool geometries considered and the machine kinematics. For example, the degree of deformation and the shoulder angle of the die have a significant influence on the local change in shape and the normal stress. The relative velocity between tool and workpiece is influenced not only by the die geometry but also by the punch velocity. Absolute values for normal stress also depend on the workpiece material.

Using FEM simulations (software: simufact.forming) a load case analysis was carried out for lubricated and dry full forward extrusion with different die geometries. The results form the basis for the selection and conception of suitable analogy tests for the formation of the tribological test sequence. The simulations were carried out under the boundary conditions of a constant punch velocity (hydraulic press, v_P = 20 mm/s) and homogeneous initial temperature distribution of 20 °C for all dies (T_T), the workpiece (T_{WP}) and the environment (T_S). To classify the load spectrum, simulations were performed under lubrication (Coulomb model, μ = 0.06, corresponding to [31]) and with high friction between tool and workpiece during dry forming (combined friction model, μ = 0.5 and m = 1). For the thermally relevant material data heat conductivity λ, density ρ and heat capacity c_p as well as for the heat transfer to the tool α_T, to the environment α_S and by radiation ε the standard values for the materials pure aluminum and the cold work steel 1.2379 were used. In cold forming,

these values are less relevant, so that a more precise experimental determination does not seem justified. The elastic material behavior was modelled at room temperature with an elastic modulus of 71 GPa and a Poisson ratio of 0.35. Extrapolated flow curves were used for the plastic material behavior [32]. The basic simulation model with its boundary conditions and material data is summarized in Figure 2.1. The workpiece is discretized with 6,500 elements (edge length 0.2 mm) at the beginning of the process and is remeshed in case of tool penetration or a local strain change of 0.4.

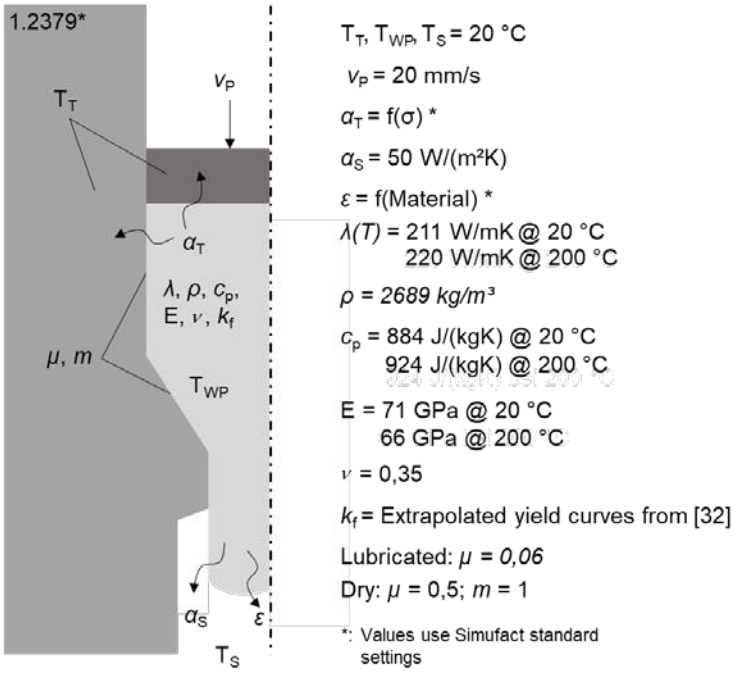

Fig. 2.1: Summary of the simulation model for the lubricated and dry full forward extrusion. [32]

The aluminum billet has a diameter of 20 mm and is 25 mm long. The die variations considered are sketched in Fig. 2.2 and differ in the degree of deformation (φ = 0.2; 0.8; 1.4) and the shoulder angle (α = 30°, 45°, 60°). The basic specifications from [33] were taken into account in the design, whereby the low degree of deformation of φ = 0.2 can be described as atypical for impact extrusion. By using this small diameter reduction, it can be checked whether there are lower degrees of deformation with reduced load spectra for which dry impact extrusion appears feasible. The die land is 2 mm long for all variants. The transition radii between the initial diameter and the shoulder (marked ① in Fig. 2.2) are 4 mm for the dies with φ = 0.8 and 1.4 and 0.75 mm for the dies with the smallest deformation φ = 0.2. Transition radii of 1 mm are incorporated in the transitions between the die shoulder and the die contact surface (marked ② in Fig. 2.2).

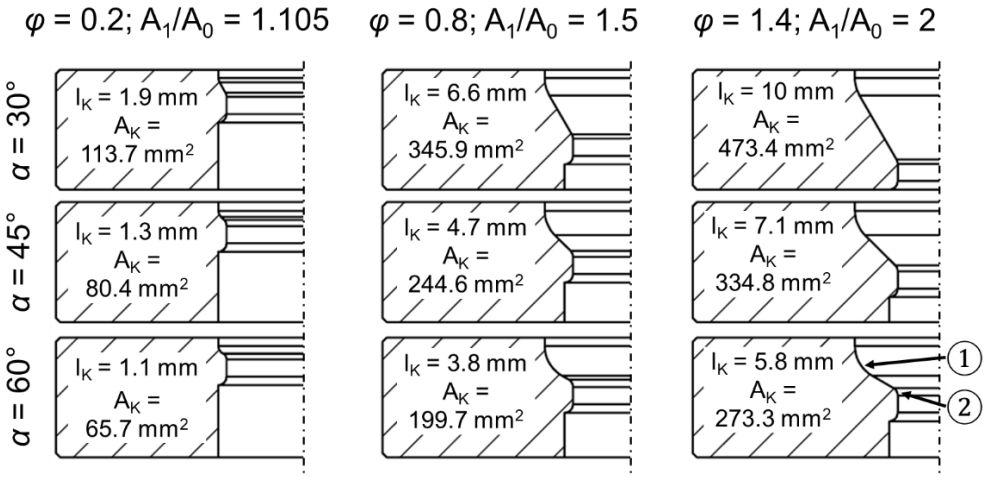

Fig. 2.2: Considered dies with variable true strain φ as well as shoulder angle α and resulting surface enlargement A_1/A_0, contact area A_K and contact length l_K in the shoulder (data without considering die contact area and transition radii ①, ②). [32]

In the following, the previously listed process variables relative contact stress, relative velocity and temperature in the contact zone are investigated as a function of the die geometry and the friction conditions. For comparability of the individual process variants, the individually considered variables of the load spectrum were normalized, if possible, depending on the workpiece material (e.g. initial flow stress) or the machine kinematics (e.g. punch velocity). This procedure enables the load spectra to be compared later in the full forward extrusion process and in the analogy tests of the tribological test sequence. The load quantities were taken along the contact zone, after 12.5 mm punch stroke or a process time of 50 %, respectively.

Figure 2.3 and 2.4 summarize the results for the individual dies and friction conditions. In order to allow for an improved comparability of these results with the dry results, the maximum limits of the axes have been chosen accordingly large. Different lengths result for the considered distance s, since the area between die and workpiece increases with a higher true strain and smaller die angle. An even more detailed process analysis, for example using elementary plasticity theory, can be found in [32].

The calculations shown here allow initial findings to be derived for the dry impact extrusion of aluminum and the associated challenges. Based on the determined load spectrum, a selection and design of the tribological test sequence is finally possible. The surface modifications to be developed, which are to substitute the lubricant in its functions, will lead to friction within the simulated interval and thus to a load spectrum between these extreme values.

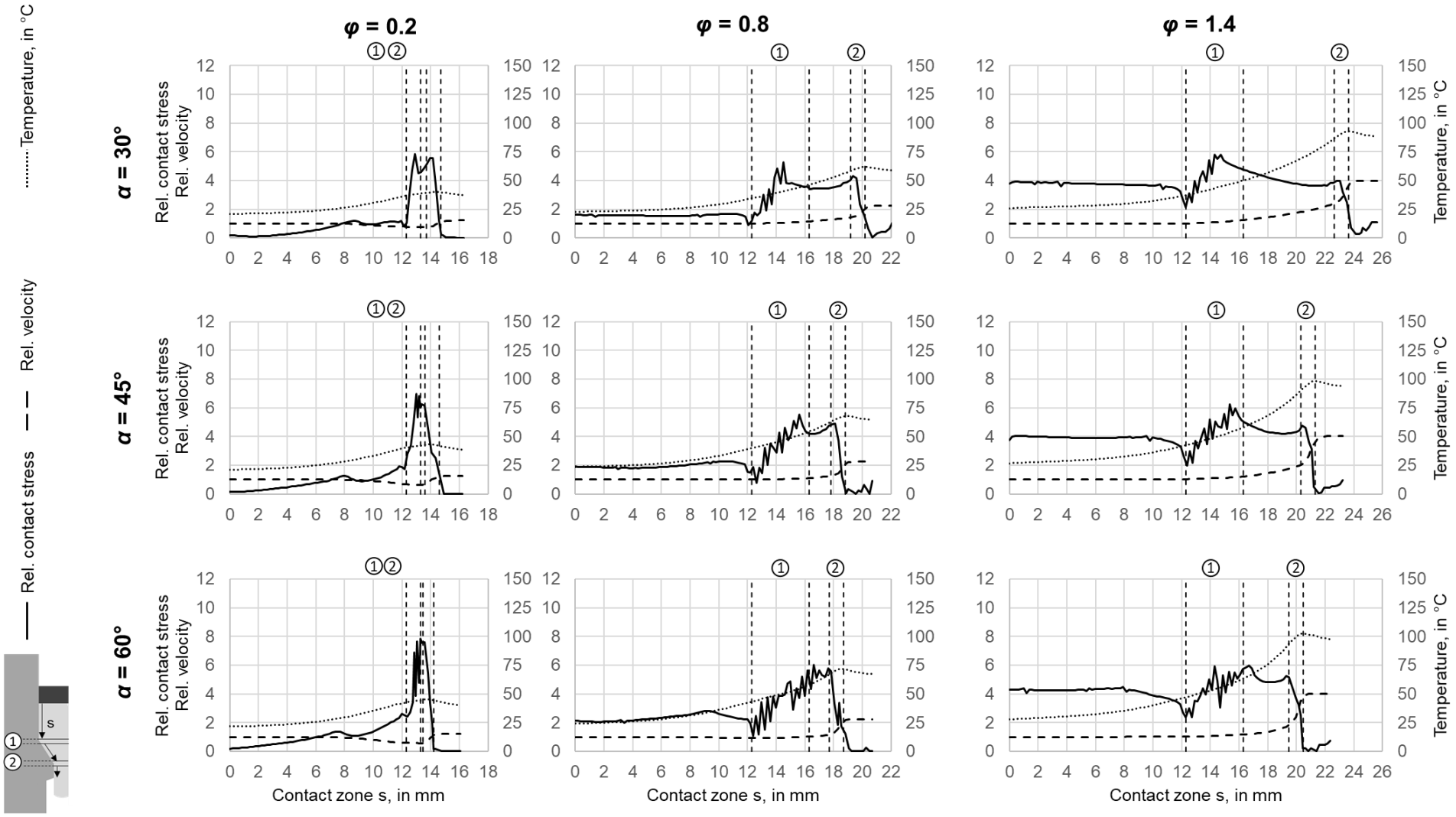

Fig. 2.3: Relative contact pressure, relative velocity and temperature occurring along the contact zone s after 12.5 mm punch stroke for different die geometries in the lubricated process. [32]

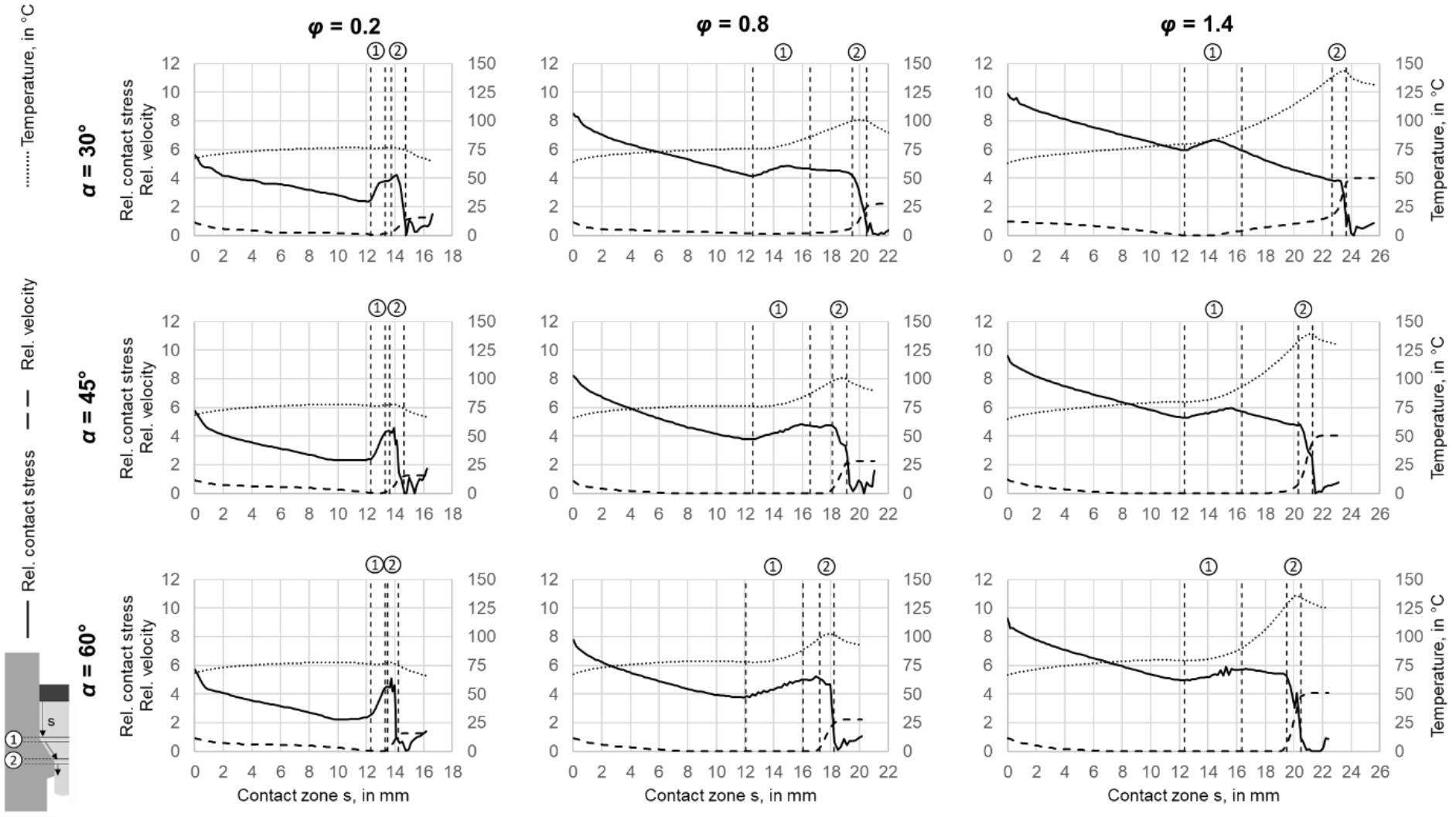

Fig. 2.4: Relative contact pressure, relative velocity and temperature occurring along the contact zone s after 12.5 mm punch stroke for different die geometries in the dry process. [32]

2.2 Tribological test sequence

A tribological test sequence with three different laboratory tests was developed based on the previously presented simulation results. The tribological test sequence includes:

1. The conical tube-upsetting test
2. A compression-torsion tribometer
3. A demonstrator test bench of full forward extrusion

This publication focuses on the last two elements of the tribological test sequence. Further information regarding the conical tube-upsetting test can be found in [32,34]. Fig. 2.5 shows the test chamber of the compression-torsion tribometer (a first version of the system was presented in [35]) for closer examination and explanation. The used motor has an effective torque of 135 Nm, so that no drop in rotational speed is to be expected even when contacting the test specimens. A high force cylinder is used to apply the axial force. Operated with up to 10 bar air pressure, forces of up to 18 kN can be generated. Clamping bushes are used for the specimen holders. Various measured variables are recorded. The measurement of the applied axial force is realized via a load cell with a maximum measuring range of 200 kN and an associated measuring amplifier. Via a lever arm the torque transmitted from the driven motor side is transferred to another load cell (measuring range up to 35 kN) and can be calculated with knowledge of the lever arm length (constant 30 mm). A measuring amplifier is also used for this purpose. On the cylinder side, a displacement transducer (potentiometer) is installed, with which the slide position can be recorded. On the driven side, the number of revolutions is measured with the aid of a speed sensor and an eight-segment encoder wheel mounted on the shaft.

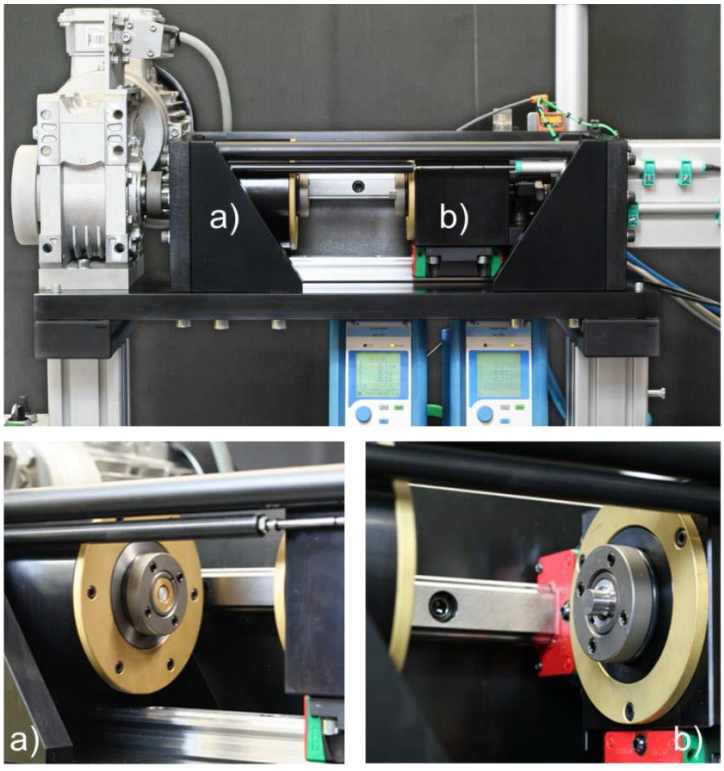

Fig. 2.5: Test chamber of the tribometer with: a) sample holders for the workpiece sample on the engine side, b) sample holders for the tool sample on the pressure cylinder side. [36]

In order to be able to map the previously determined load spectrum, special specimens must be used. Figure 2.6 shows the developed specimens. The brass encapsulation ring used keeps the workpiece material in permanent contact with the counter body, so that normal pressures above the initial flow stress can also be tested with defined sample geometry. The workpiece specimen can be deformed by the free space to the encapsulation ring. In this way, conditions at the die shoulder are reproduced. The represented size of the free space corresponds to a doubling of the contact area. By dimensioning the free space differently, other surface enlargements can also be realized. A heterogeneous relative velocity occurs over the contact radius. This circumstance must be taken into account in the evaluation of the test. Deviations in shape must be prevented during the production of the specimens. Otherwise, influences on the measurements cannot be excluded [37].

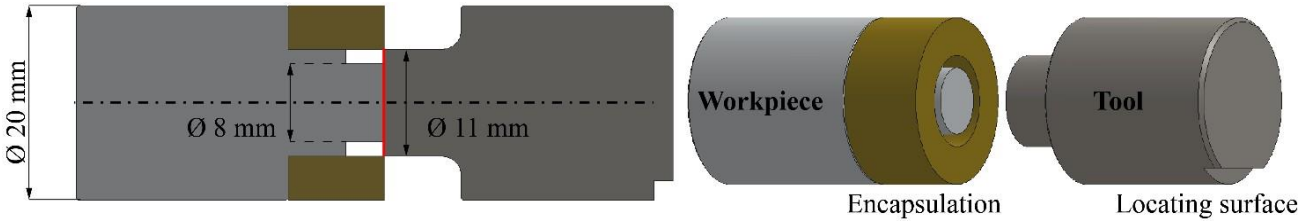

Fig. 2.6: Design of the used workpiece and tool specimen with encapsulation ring and locating surface in sectional and full view; final contact area in red [38]

The final evaluation of the tribology of dry impact extrusion is done in a laboratory extrusion test (first presented in [39]). This completes the test sequence and brings the testing procedure even closer to the industrial production. The requirements for the test stand include the possibility of testing different die geometries and the accessibility of the die surfaces for the processing of the surface layer. Furthermore, the surfaces must be suitable for the subsequent wear analysis and the tool costs must be controllable.

Horizontally split dies are used to meet the above requirements. This ensures the required accessibility for machining and wear analysis. Furthermore, individual tool segments can be used several times. For the selection of split dies, the reduction of stress peaks in the transition radii plays only a minor role. When processing pure aluminum, the forces occurring are sufficiently low so that this type of damage does not occur. The demonstrator test rig and the individual tool segments are illustrated in Fig. 2.7. The three die segments (die holder, die and recipient) are inserted into the container and axially clamped by the container lid. The container is connected to the base plate by the fastening clip. Despite the small clearance between punch and die and despite the axial pretensioning of the entire package, there is a small axial flow of material against the punch stroke and in transverse direction between die and container. Due to the possibility to remove the complete package from the container, the cross flow is unproblematic. However, the axial material flow can lead to high tensile forces when the punch is pulled out. For this reason, the punch is designed in such a way that a breakage occurs at the punch head if the tensile forces are too high and the entire structure of the demonstrator tool is not subjected to excessive tensile forces. The guidance of the punch plate is ensured by the four guide pillars between base plate and top plate. The entire setup was tested with dies according to Fig. 2.2 and reference curves for lubricated and dry tests were recorded and presented in [32,40].

The tribological test sequence developed forms the basis for the experimental characterization of novel surface layers for dry forming. Starting with the simulative and analytical investigation of impact extrusion, as the first element of the test sequence, the requirements for the laboratory tests to be developed were determined and in the following second element of the tribological test sequence a compression-torsion tribometer was designed. By using encapsulated test specimens, high relative contact pressures can be achieved, as in impact extrusion of aluminum. A free space in the test specimen also results in a sufficient surface enlargement so that the oxide layer on the aluminum body is broken up in the contact area. As the third and last element in the tribological test sequence, a laboratory-scale demonstrator test rig was designed. Horizontally split dies allow a specific processing of the die segments and individual components can be used again.

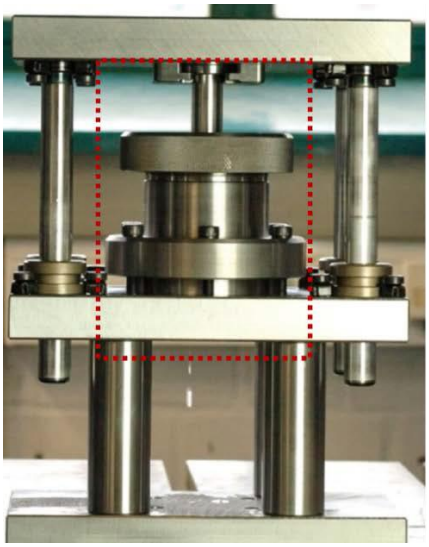

Active elements:
1. Punch
2. Recipient
3. Die
4. Billet

Passive elements:
5. Die holder
6. Punch plate
7. Container lid
8. Container
9. Fastening clip
10. Base plate

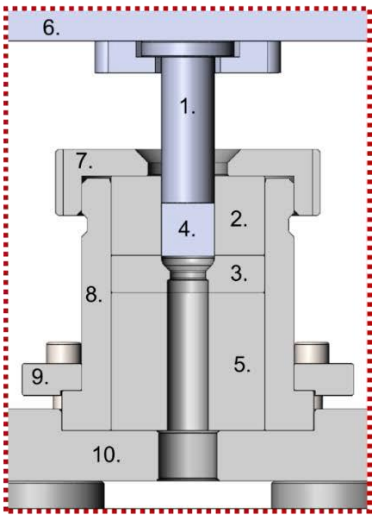

3 Surface structuring and polishing

As stated in section 1, the surface topography of the tool plays an important role in the tribological system of dry cold extrusion of aluminum. Three different laser remelting processes were used to investigate the influence of different surface modifications on the adhesive wear behavior in this system. In all three processes a focused laser beam creates micro melt pools on the metal while it is scanned over the surface. Depending on the process parameters the surface topography can be smoothened (polished) and/or new structures can be created. In contrast to other polishing or structuring technologies the material is only redistributed instead of removed or added.

In laser micro polishing pulsed laser radiation is used to create shallow melt pools on the metal surface which have approximately the same lateral dimensions as the laser spot but are only a few micrometers deep, as depicted in Fig 3.1b. These shallow melt pools solidify before the following laser pulse creates the next one. Due to their low remelting depth and short duration of existence only the micro roughness with wavelengths below approx. 10 µm is smoothened by the surface tension of the melt while larger surface structures are preserved [41]. This process can be applied on its own on less rough surfaces but often complements the other two laser remelting processes (explained in the following) as a finishing step.

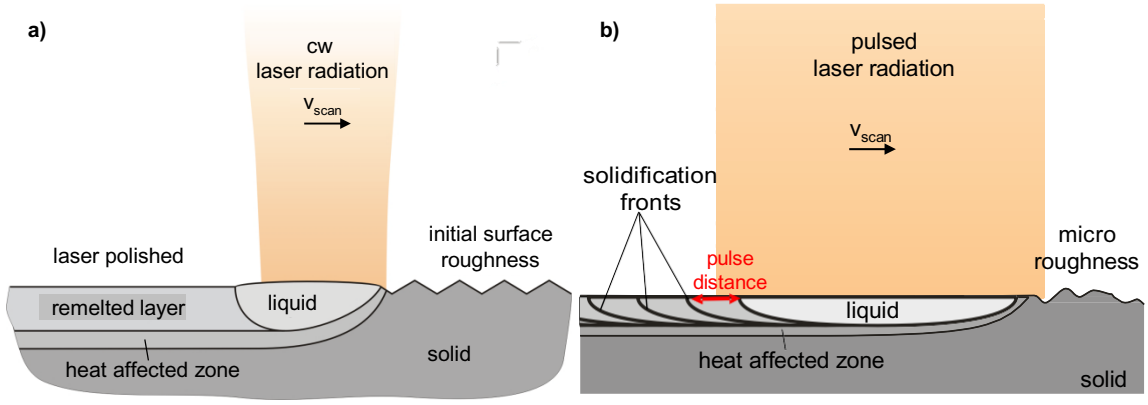

Fig. 3.1: Process principle of the laser polishing process: a) macro laser polishing with continuous wave laser radiation; b) micro laser polishing with pulsed laser radiation. [41]

Laser macro polishing on the other hand uses continuous wave laser radiation to create a continuous melt pool with larger remelting depths of 20 to 100 µm. This process can even out surface structures that are larger in height and wavelength and thus smoothen the whole roughness spectrum [41].

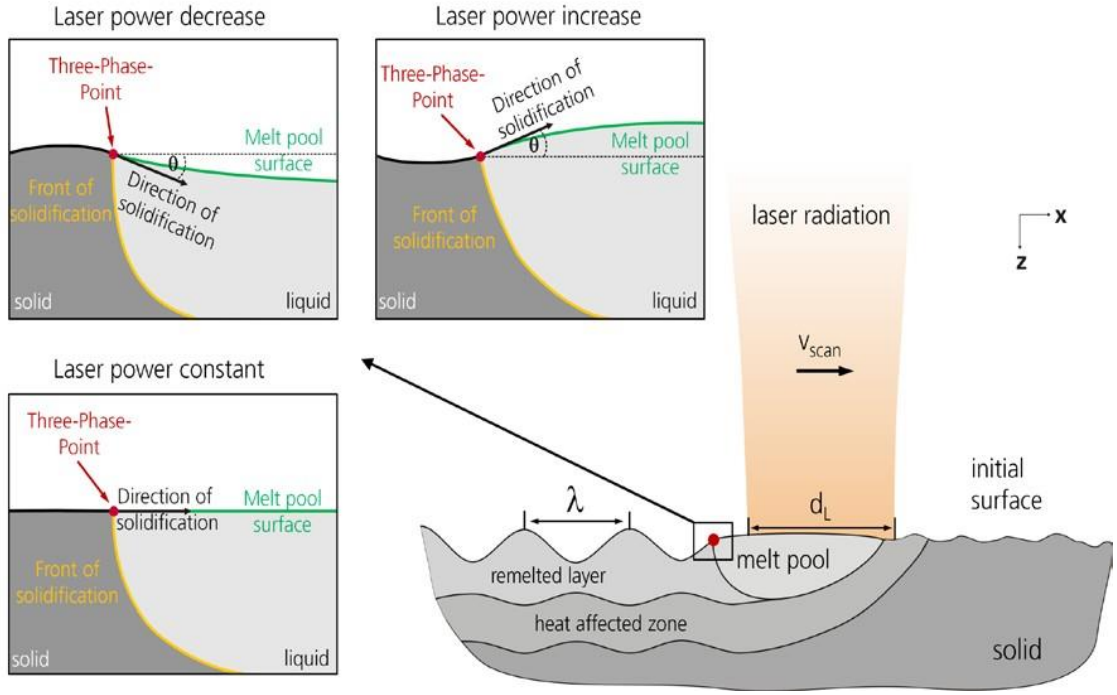

The third laser remelting process investigated here is surface structuring by laser remelting (SSLRM). This innovative process is similar to laser macro polishing but instead of keeping the laser power constant it is modulated sinusoidally. This power modulation creates periodically increasing and decreasing melt pools, which redistributes the molten material and results in the creation of continuous periodical hill and valley (sinusoidal) structures as depicted in Fig 3.2 [42].

Since the structures are created directly from the melt, the surface roughness is similar to macro laser polishing. Compared to conventional polishing and grinding all three laser remelting processes have the potential tribological advantage that they create smoother surface topographies without sharp edges, grooves or burrs, as can be seen in Fig 3.3. Especially in dry metal forming this is thought to be beneficial because without a lubrication film there is more direct contact between tool and workpiece.

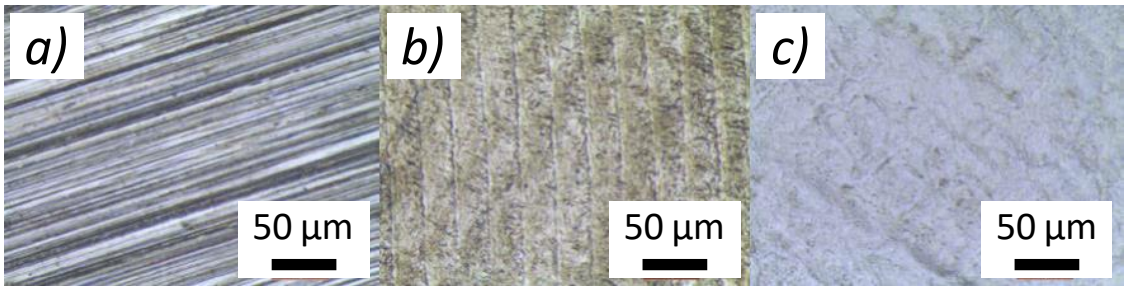

Fig. 3.3: Microscopic images of ground (a), macro laser polished (b) and micro laser polished (c) surface of tool steel 1.2343. [43]

All three laser remelting processes have in common that due to the rapid cooling of the micro melt pool the material solidifies homogeneously with a very fine-grained microstructure. Therefore depending on the material and initial state, often an increase in hardness can be observed. Together these processes allow to selectively smoothen the surface in various parts of the roughness spectrum as well as creating stochastic or directed structures ranging from µm to mm in height and wavelength.

Initial investigations comprised the micro laser polishing of hot work tool steel AISI H11 (1.2343) in two different qualities – standard quality and electro-slag remelted (ESR) quality [38]. This steel was chosen as a reference because the development of the laser polishing process at this point was largely carried out on this material. These first results showed that smoother surfaces achievable on the higher grade ESR steel required lower forces on the above mentioned tribometer and result in less measurable aluminum adhesion compared to the rougher surface created on the standard quality steel due to inhomogeneities in the standard quality material.

These investigations where extended to macro laser polishing and to include the cold work tool steel AISI D2 (1.2379) which is commonly used for the cold extrusion of aluminum. Process parameters had to be developed for the laser polishing of this material. For both materials the mean roughness could be decreased from Ra = 0.5 µm on the ground initial state to Ra = 0.2 µm. The macro laser polishing, which smoothened the surface in the meso roughness range of the roughness spectrum (spatial wavelengths $5 < \lambda < 160$ µm) had little to no influence on the aluminum adhesion compared to the initial state. Micro laser polished surfaces on the other hand yielded improved wear behavior with less adhered aluminum [43]. Their significantly reduced micro roughness (spatial wavelengths $\lambda < 5$ µm) firstly suggested that microstructures play an important role in the formation of aluminum adhesion. The combination of macro laser polishing followed by micro laser polishing yielded the best results, i.e. the adhered aluminum could be reduced by a factor of 10 compared to the ground initial state [43].

In order to test these findings under real world conditions a concept was developed to apply the laser polishing process to the 3D-surface of a die for aluminum cold extrusion (see part 3. in Fig 2.7). The laser polishing process was adapted to sloped surfaces of AISI D2 and executed on a 3D capable laser polishing machine at LLT using the available CAD CAM process chain to generate scan paths on the 3D CAD model of the die. The laser polishing process is executed by using the 3 optical scanning axes of the laser scanning system simultaneously with 5 mechanical axes to position the workpiece. This enables a continuous polishing process without the need to stitch multiple patches for macro as well as micro laser polishing [40].

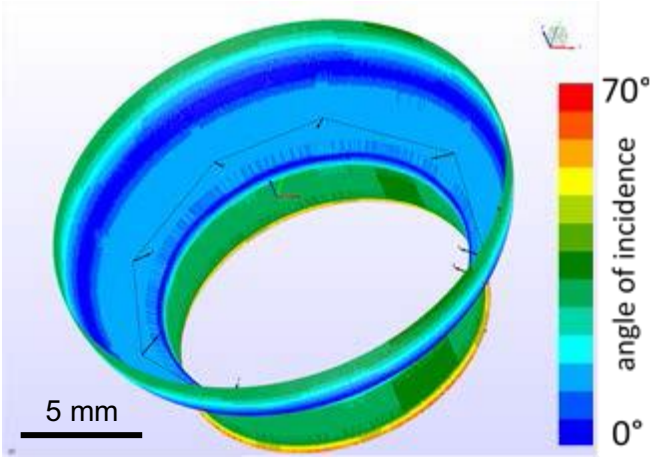

Fig. 3.4: 3D Laser scan paths on extrusion die. False color coding showing angles of incidence. [40]

The three laser remelting processes were investigated on a more homogeneous powder metallurgically melted variant of AISI D2 (i.e. AISI D2 PM or 1.2379+) [44, 45] and process parameters were developed. This third material was added to the investigation, as large inhomogenities (chromium carbides) in the standard variant were found to influence the coating process negatively (see section 4). It could be shown that the macro laser polishing process is able to homogenize the thin remolten surface layer, thereby eliminating the chromium carbides in this region, as depicted in Fig 3.5 [46].

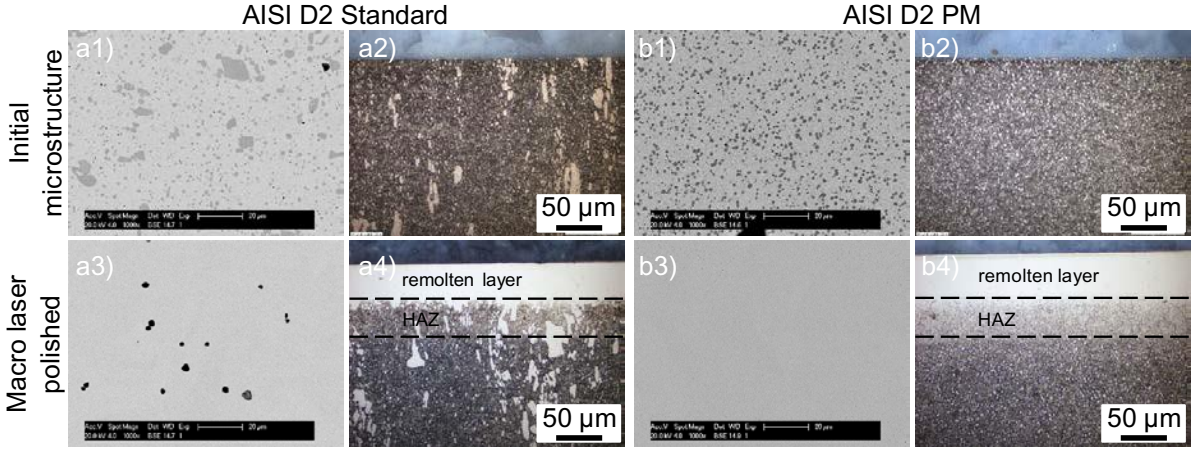

Fig. 3.5: SEM and light microscope images of a) AISI D2 Standard and b) AISI D2 PM specimen: manually polished surface (1) and cross-section (2) of the initial microstructure; manually polished surface (3) and cross-section (4) of a macro laser polished specimen. [46]

In order to investigate the influence of larger scale surface structures on the problem of aluminum adhesion the process of surface structuring by laser remelting was developed on the two tool steels to create circular structures (star shaped and concentric rings) of several 100 µm wavelength and several µm structure height (smallest possible structure dimensions on available laser machine) on the tribometer test surfaces. These structures were chosen to place the sinusoidal wave structure in direction of as well as perpendicular to the material flow generated on the tribometer. Due to the working principle of the structuring process the target structure determines the required laser scanning strategy, i.e. a spiraling scanning of the laser is needed to create a star shaped structure while a rotating pendulum scanning creates the concentric circle structure. These scanning strategies were implemented in the laser scanner control software by separate script and parameters were developed to create the target structures. The tribological results are discussed in section 5.

A similar script was developed to create the final structure on the 3D surface of extrusion dies made from 1.2379+ for final real world testing. Due to the accessibility of the die the laser structuring needed to be performed with angles of incidence equal to the slope angles of the dies (30°, 45°, 60°) (see Fig 3.6). The process had so far only been applied to flat 2D surfaces with perpendicular angle of incidence. Therefore the structuring process was developed on sloped surfaces to determine parameters for the target structure under different angles of incidence. Additionally the patching of structured fields was investigated to identify process strategies for seamless structure continuation in cases where surfaces cannot be structured in one process step.

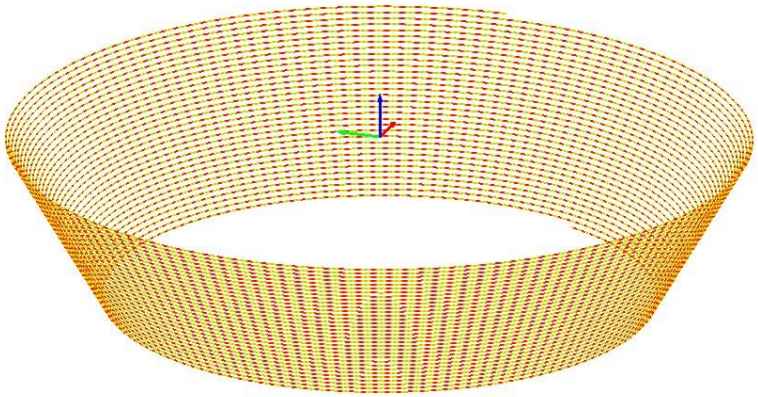

Fig. 3.6: 3D representation of the programmed laser scanning path spiraling down the cone of the extrusion die to create the wave structure. Colors represent laser power modulation.

Finally the findings for the different processes were combined to minimize interaction of the aluminum with the tool during cold extrusion. Therefore the recipient as well as the straight walls of the extrusion die were macro laser polished to smoothen the turning grooves. The sloped shoulder of the die, where the aluminum is deformed, was also macro laser polished to smoothen the initial state for the subsequent structuring by laser remelting. All laser remelted areas were finished with laser micro polishing to smoothen micro structures resulting from the remelting with continuous laser radiation (see section 5). The effects of the different process steps on the surface topography are displayed in Fig. 3.8. The initial surface after turning shows turning grooves with a height of several micrometers. This is the same height range as the target wave structure. Therefore the first macro laser polishing step homogenizes and smoothens this rough surface (Fig. 3.8 middle) to prepare it for the structuring by laser remelting step, which creates a wave structure with a wavelength of 300 to 400 µm and an amplitude of ca. 1 µm.

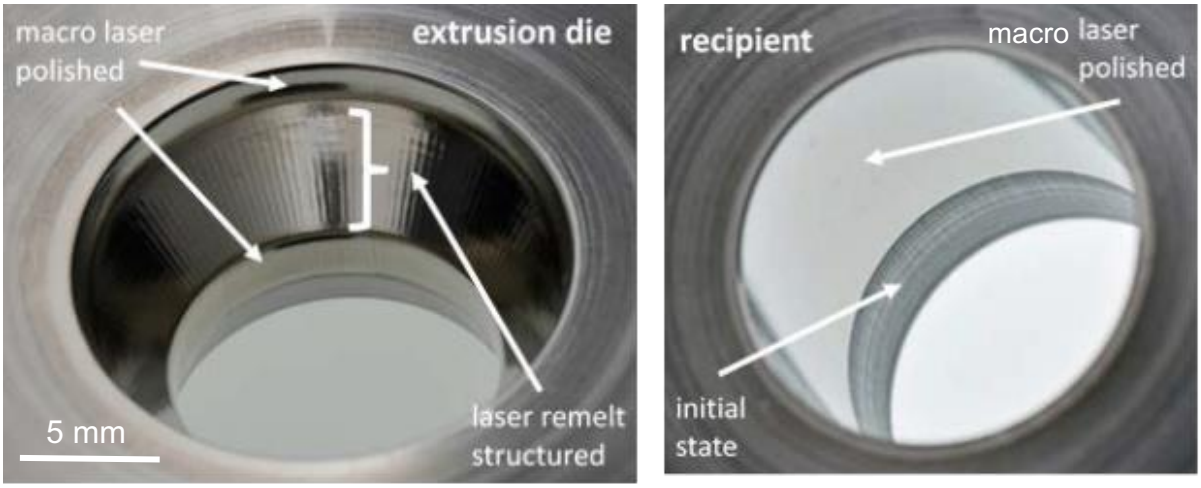

Fig. 3.7: Left: extrusion die - laser polished and structured. Right: recipient - inside partially laser polished in aluminum contact area.

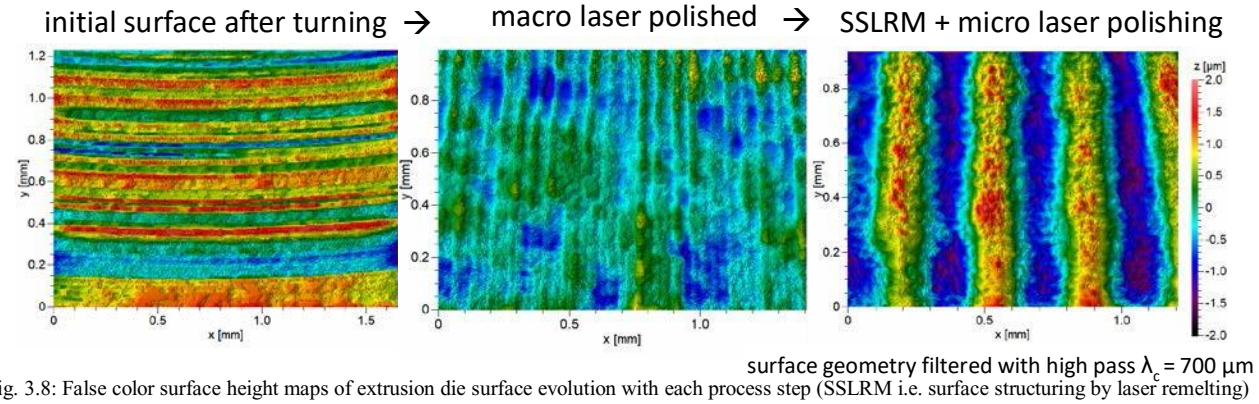

Fig. 3.8: False color surface height maps of extrusion die surface evolution with each process step (SSLRM i.e. surface structuring by laser remelting)

4 Coating and functionalization

As emphasized in section 1, it is the aim of this chapter to design and synthesize coatings suitable to reduce aluminum adhesion and to protect the forming tool against wear. The absence of liquid lubricants in cold extrusion of aluminum results in macroscopic aluminum adhesion and a continuous degradation of the tool surface as observed in Figure 4.1. An EDX line-scan (Figure 4.1b) across the interface of an adhering particle (Figure 4.1a) indicates the role of surface oxides on the tool involved in the aluminum adhesion [47] as investigated by [9]. Hence a protective coating is necessary to avoid aluminum adhesion and to shield the tool surface from degradation. The first choice fell on Mo_2BC as coating material. Discovered in systematic studies of transition-metal boron carbides by quantum mechanical ab initio studies [48, 49], the nanolaminated Mo_2BC bares the unusual combination of a very stiff and moderately ductile material. Its fracture resistance was determined experimentally by in-situ straining experiments outperforming other protective tool coatings, e.g. TiAlN, and characterized close to the ductile behavior of metals [50].

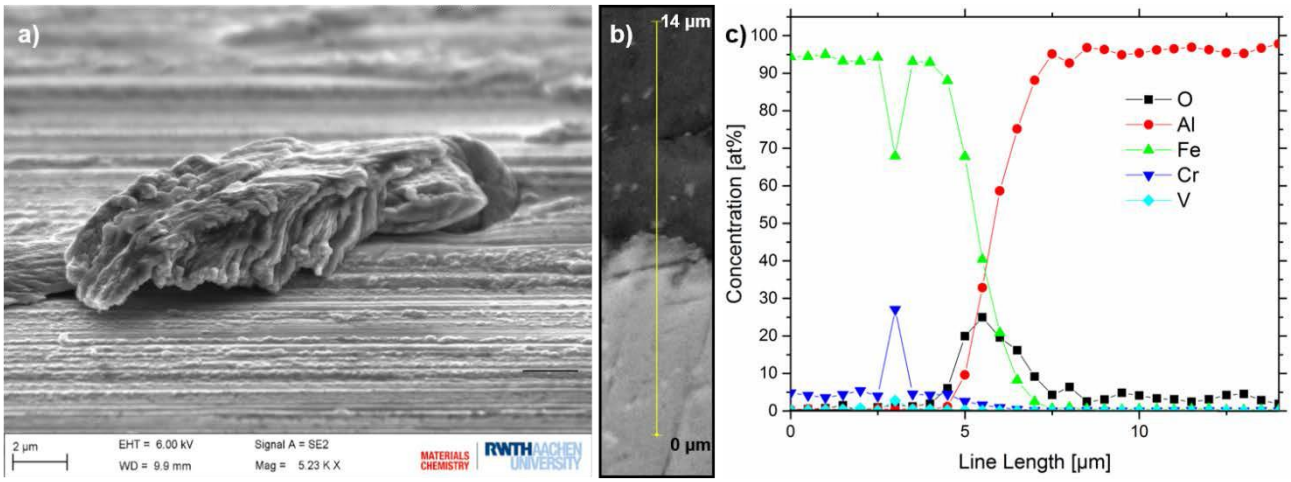

Fig. 4.1: Aluminum adhesion on tool steel after testing in the tribometer, (a) secondary electron micrograph of adhering particle, (b) polished cross-section of aluminum-steel interface for EDX line-scan in (c). Reproduced from [47], with permission of AIP Publishing.

As first measure, the coating process adapted from ceramic substrates was adjusted for hardened tool steels. Specifically, the substrate temperature during deposition was lowered to prevent hardness losses. High power pulsed magnetron sputtering was utilized to ensure the crystal quality of the Mo_2BC film at the lowered growth temperatures down to 350°C [49]. Parallel, the interaction of Mo_2BC with aluminum was investigated by theoretical means employing quantum-mechanical ab-initio methods for studying the hard-accessible nature of aluminum adhesion at the tool-workpiece interface. In a theoretical experiment performed with the openMX and VASP simulation packages, nine aluminum atoms were set in the proximity of a pristine or oxidized Mo_2BC resembling the structure of a deformed aluminum crystal (Figure 4.2a). Structural optimization based on energy minimization revealed shrunken distances between Al and (oxidized) Mo_2BC surfaces as well as the formation of aluminum bonds with the (oxidized) Mo_2BC surface (Figure 4.2b) [51,52]. Moreover, the adsorption energy per adsorbed aluminum atom was determined on both surfaces, pristine and oxidized Mo_2BC, and compared to the adsorption energy of well-studied other pairings. Evidently, the adsorption energy of aluminum on pristine and oxidized Mo_2BC obtained as 4.31 and 4.36 eV/atom locates within the range of other adsorbants firmly attached by ionic or covalent bonds [52]. Conclusively, the theoretical studies revealed the atomic onset of aluminum adhesion as it can be expected that the material flow in aluminum forging will lead to shearing within the aluminum work material due to the higher plasticity of the metallic aluminum causing aluminum remaining chemically attached to the surface of the coating. Moreover, analyzing the adsorption energy qualitatively suggests the necessity of a tool surface terminated by van-der-Waals interactions for low adsorption and adhesion.

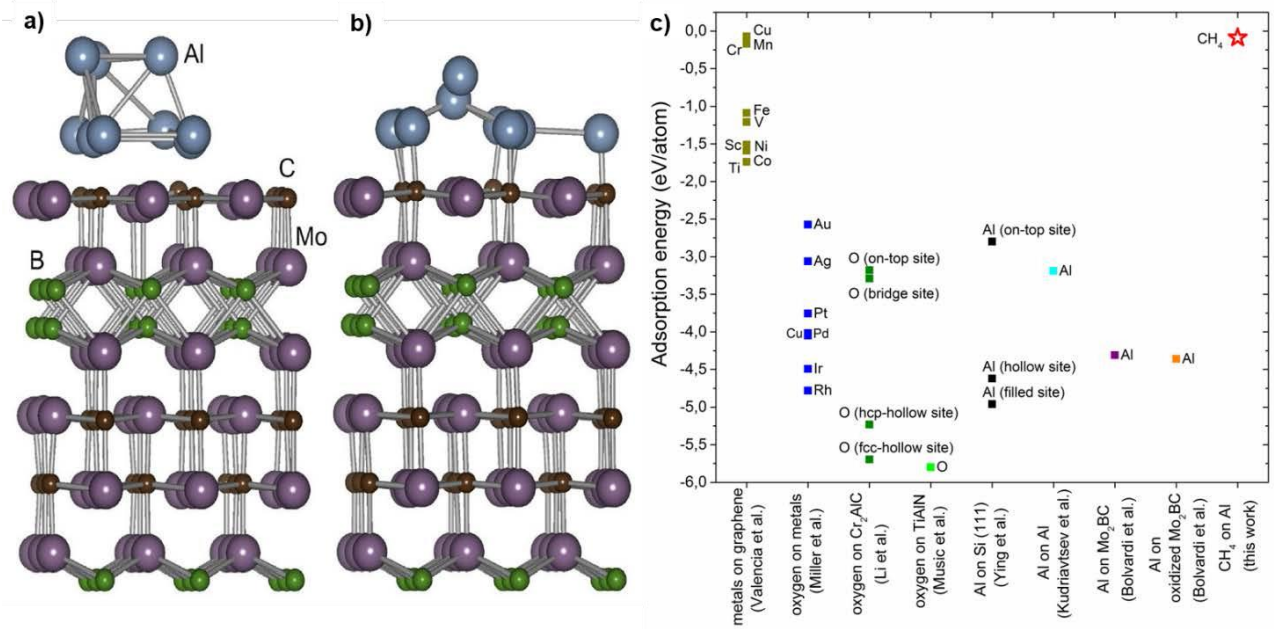

Fig. 4.2: Surfaces of Mo_2BC exposed to aluminum in initial (a) and final (b) structure of theoretical experiment [51] and comparison of adsorption energies (c). [52]

Essentially, the results of the atomistic modelling on aluminum adhesion demand a strategy change towards tool surfaces functionalized by alkyl moieties similar to adsorbed additives on tool steel surfaces exposed to liquid lubricants [53]. In this regard, the term surface functionalization refers to the assembly of a monolayer (ML) of alkyl phosphonic acids, thiols or silanes on surfaces of metals or metal oxides. Hence, these surfaces are altered by terminating them with distal alkyl moieties [54]. Specifically, functionalization of metal oxide surfaces with alkyl phosphonic acid was reported to result in monolayers firmly attached to the surface by up to three P-O-M (M = metals) bonds and a dense arrangement of alkyl chains for moieties with more than 8 carbon atoms [55,56]. In order to apply alkyl phosphonic acid monolayers on forming tools homogeneously, a vacuum process was designed in a newly self-build set-up where n-octadecylphosphonic acid (C18PA) was evaporated on the surface of polished tools (Figure 4.3a). A subsequent substrate annealing lead to the removal of physisorbed molecules and the formation of the phosphonic acid monolayer [57]. The complete process took place in a vacuum chamber at pressures of $1 \cdot 10^{-4}$ Pa. The resulting monolayer assesses 2.5 nm approximately [58] and was characterized by x-ray photoelectron spectroscopy (XPS) detecting the P-O-M bonds in both, the O 1s and P 2p signal (Figure 4.3b, c) [57,59].

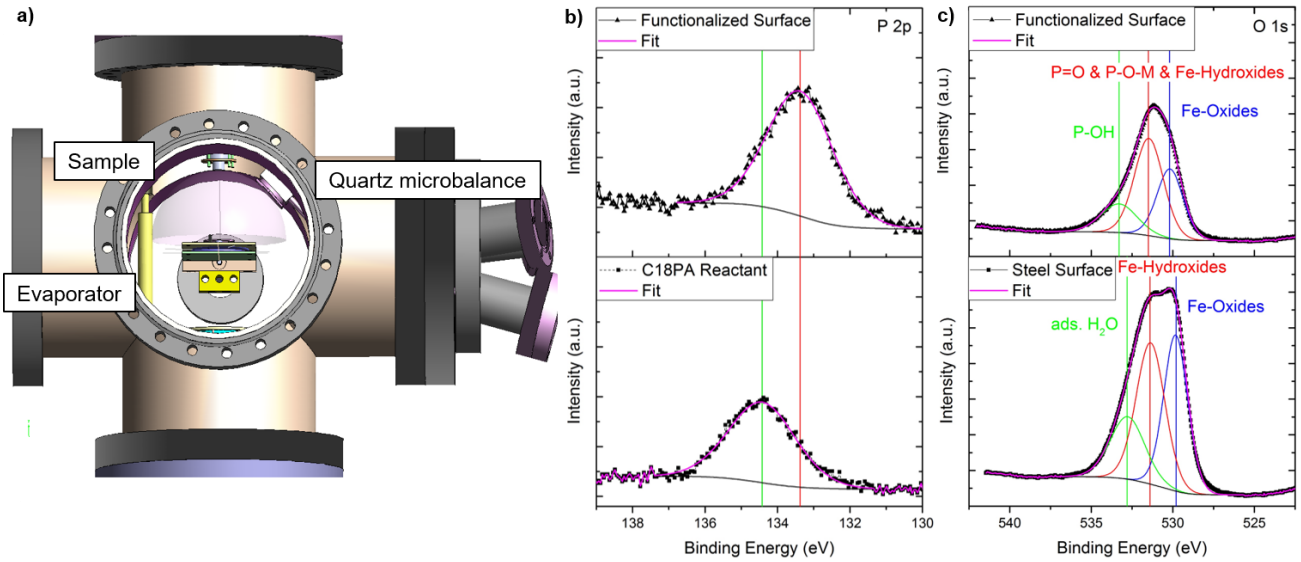

Fig. 4.3: Experimental set-up (a) and photoelectron spectra of functionalized 1.2343 proving the formation of P-O-M anchoring the C18PA monolayer to the 1.2343 surface in phosphorous (b) and oxygen (c) signals. Reproduced from [57], with permission of the American Vacuum Society.

Subsequently, manually polished tools manufactured of hardened 1.2343 and 1.2379 tool steel were functionalized as described above and tested in the tribometer. The results depicted in Figure 4.4 reveal a strong reduction of transferred torque comparing the functionalized tool made of 1.2343 to the non-functionalized reference. As described in chapter 2, the quantity of transferred torque serves in this experiment as an integral measure of the interaction between tool and aluminum workpiece [47,57]. The experiments carried out with 1.2379 tool steels show a different behavior compared to the 1.2343, as no significant reduction in transferred torque is measured comparing the functionalized 1.2379 tool steel with the reference [47]. After the experiment, the volume of adhering aluminum on the tools was determined utilizing white-light interferometry (WLI) subtracting the untested surface from the tested surface. The results clearly indicate an adhesion reduction for the functionalized 1.2343 of around 60 % compared to the reference, while functionalization of the 1.2379 surfaces results in a less pronounced adhesion reduction. In order to understand the difference in functionalization of the two tool steels, the microstructure as well as the local surface chemistry of the functionalized steels was determined by electron microscopy and auger electron spectroscopy (AES).

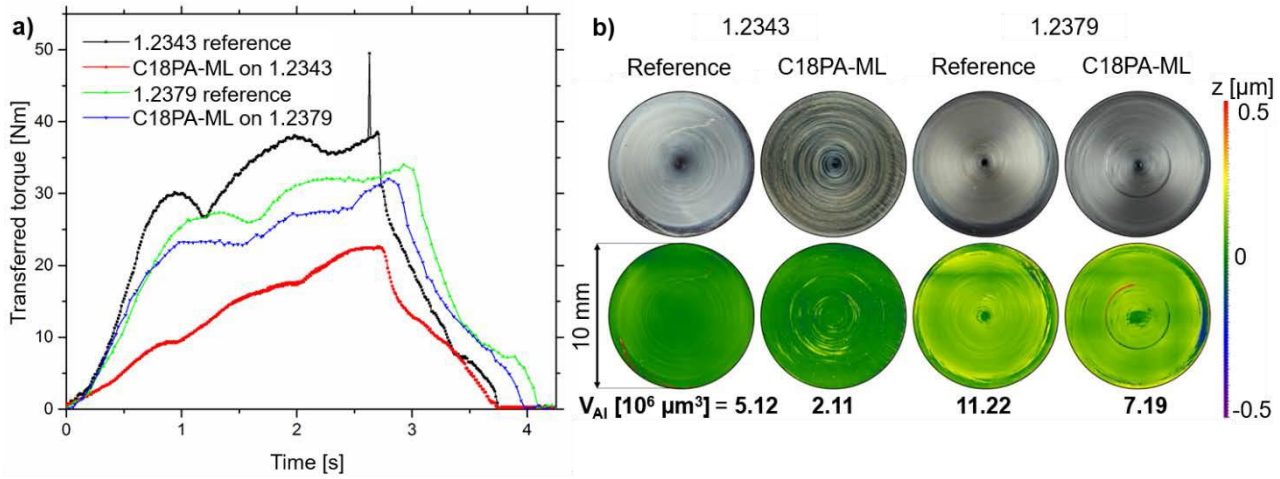

Fig. 4.4: Functionalized tool steel surfaces tested in tribometer where transferred torque (a) between tool and workpiece was measured during workpiece deformation and aluminum adhesion was determined by WLI (b) of the tool surfaces after the test. First row in (b): Photographs of tool surface, second row in (b): Height deviation due to aluminum adhesion. Reproduced from [47], with permission of AIP Publishing.

While the 1.2343 steel consists of few mostly manganese carbide precipitations, the microstructure of the utilized 1.2379 tool steel reveals large chromium carbide precipitations (Figure 4.5b). Exploring the local surface chemistry by AES, phosphorous concentrations and the concentration ratios of phosphorous to metal were significantly smaller on the chromium carbide precipitations compared to the steel matrix and the more homogenous 1.2343 [47]. The concentration ratio of phosphorous to metal provides an accessible magnitude to describe the molecular coverage of the C18PA anchored by P-O-M bonds. Conclusively, the molecular coverage depends on the surface chemistry of the substrate to functionalize with C18PA.

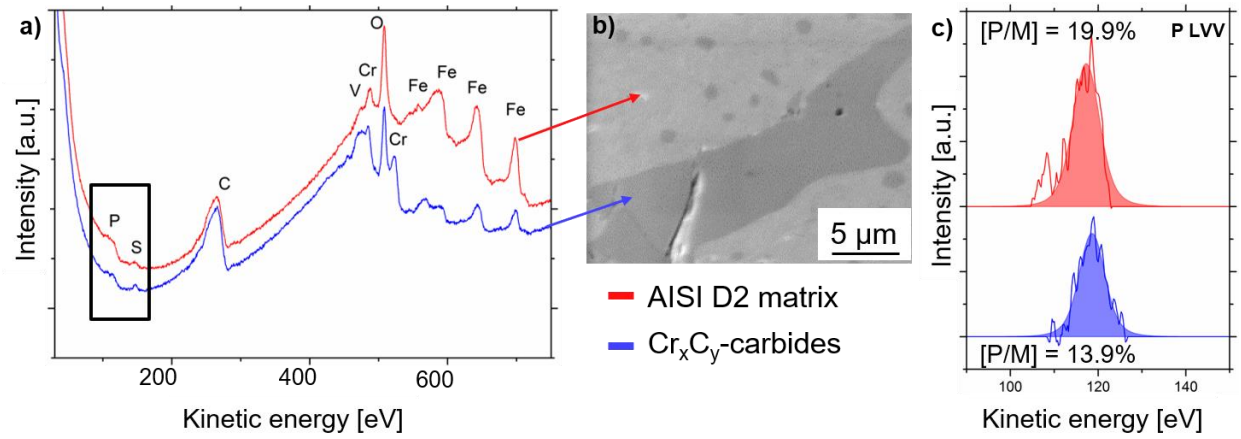

Fig. 4.5: Auger electron spectra (a,c) determined on indicated spots in electron micrograph (b). Lateral measuring spot size: <100 nm. High resolution spectra of P LVV signal (c) reveals higher phosphorous concentration on steel matrix than on carbide precipitation identified by overview spectra (a). Reproduced from [47], with permission of AIP Publishing.

As indicated by the retrieved results in [47], a reduced molecular coverage is detrimental for protection against aluminum adhesion due to the more tilted molecules and hence thinner molecular layers of C18PA. Furthermore, oxides of different metals react differently with C18PA. Especially oxides on pure chromium, molybdenum, and manganese were reported to show little or small reaction with phosphonic acids [60]. In order to overcome the difficulty of an inhomogeneous surface chemistry alongside with elements not reacting with phosphonic acids, an intermediate adhesion layer was implemented in the functionalization strategy directly coated on the tool steel surface. 20 nm thick coatings of Cu and Fe were applied as adhesion layer due to the formation of hydroxides on their oxide scale which are necessary for the chemical reaction of the phosphonic acid with the surface. The surface of these adhesion layers coated on steel disks was then functionalized with monolayers of phosphonic acids with different molecular coverages realized by a variation of the evaporation time and confirmed by P/Cu or P/Fe concentration ratios determined by XPS [59]. In a ball-on-disk set-up against aluminum, the functionalized Cu-surfaces revealed reduced friction for a certain sliding distance depending on their coverage and a reduced wear track width (Fig. 4.6a). The influence of the increased coverage on the sliding wear behavior evidences as for the functionalized surfaces with largest molecular coverage no breakdown of the lubricating effect was observed and the formation of a wear track was obstructed (Fig. 4.6b).

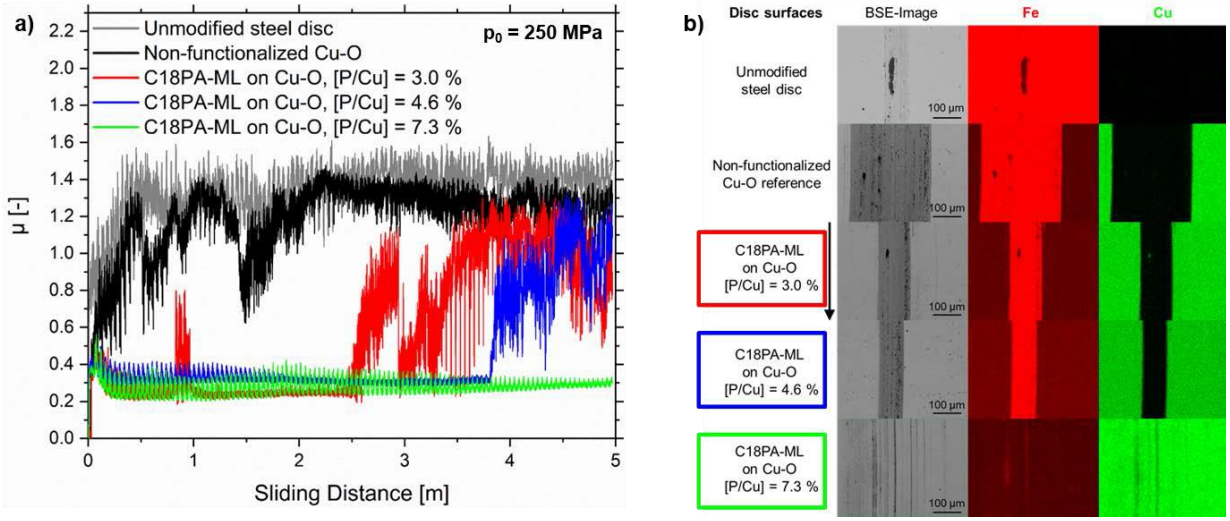

Fig. 4.6: Ball-on-disk test results of functionalized Cu-coated disks against aluminum balls. The highest coverage indicated by the P/Cu-concentration ratio revealed low friction (a) for the complete test and obstructed a wear track formation (b). [59]

Contrarily, the functionalized Fe-surfaces did not improve the sliding wear behavior of aluminum rubbing against the functionalized surfaces compared to non-functionalized and references surfaces featuring friction coefficients of μ = 1.0 - 1.4 and equal wear track widths independently of coverages. This observation lead to further investigations of the differences between the sputter coated Cu and Fe-adhesion layers, since similar coverages were measured for both, Cu and Fe-adhesion layers. Investigation of their surface chemistry revealed a significant difference in the hydroxide content of their oxide scales. As hydroxides provide a reactive side to form P-O-M bonds anchoring the C18PA molecules on the surface, the hydroxide/oxide ratio is crucial for the surface functionalization. Hence, it can be assumed, that a 2-fold decrease in the hydroxide/oxide-ratio observed for the Fe-coated surface compared to the Cu-surface dramatically influences the chemical binding situation of the C18PA molecules leading to a monolayer with less P-O-M bonds compared to the monolayers on the Cu-surface. Consequently, the sliding wear behavior is affected, as the weaker anchored molecules can be stripped resulting in direct failure upon contact of the functionalization of sputter coated Fe-surfaces.

Alternatively, a different approach was chosen to gain a homogenous surface chemistry by laser modification of utilized tool steels. Laser polishing processes (section 3) for removal of detrimental carbide precipitations as described before and laser structuring processes were also investigated regarding their influence on the formed oxide scale and the provision of reactive sides. The laser polishing of 1.2379 resulted in a slag like oxide scale consisting of several slag forming elements, e.g. Al and Si and was hence disregarded for further experiments [46]. However, 1.2343 purified by electro-slag remelting (ESR) and laser structured (section 3) surfaces revealed a sufficient number of hydroxides in the oxide scale. The combination of laser structuring and surface functionalization was tested on the tribometer tool surfaces of 1.2343 (ESR) will be further discussed in section 5 as one of the selected lubricant-free tribology concepts.

Conclusively, it was demonstrated that the functionalization of tool surfaces reduces the interaction between tool and aluminum workpiece due to the weak van-der-Waals interaction between distal alkyl-chains of functionalization and bare aluminum once the workpiece was deformed and hence dismantled from its protective oxide scale. The efficiency of C18PA monolayers as wear protection bases on two fundamental parameters: First local surface chemistry measurements revealed the importance of firm anchoring for the C18PA monolayer reducing wear protection if not chemically bound [47]. In consequence, strategies were elaborated to create a homogenous surface chemistry either by coating [59] or laser processing [61]. The combination of laser structuring and surface functionalization established so far the best working surface to prevent adhesion [62]. Further investigations on the sliding wear behavior of functionalized surfaces lead to the identification of a second fundamental parameter, which is the molecular coverage of the functionalization. Improving the molecular coverage by increasing functionalization time resulted in further reduction of friction and wear against aluminum [59].

5 Combination of laser surface treatment and functionalization

Finally, both strategies (laser processing and functionalization of the surface) were used together and the surfaces produced were tribologically characterized.

As already emphasized in section 3 and 4, some laser remelted surfaces can be functionalized with higher coverage due to increased number of hydroxides and dissolving of carbide precipitations [46]. Consequently, tribometer tool surfaces of 1.2343 (ESR) were patterned with circular and star-shaped structures of both, 1 and 10 µm structure height, as can be seen in Fig. 5.1 [62].

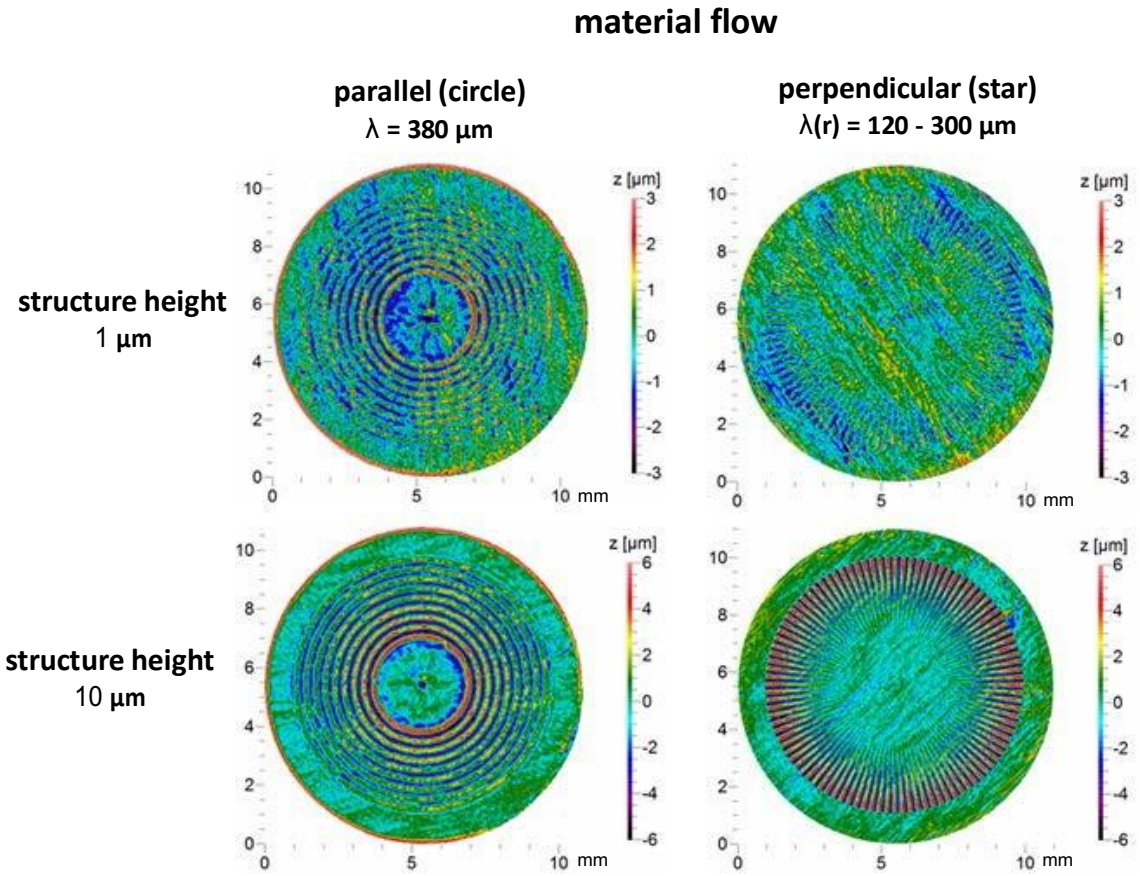

Fig. 5.1: False color representation of WLI measurements of structures created on tribometer samples with laser remelting process (SSLRM). Structures are oriented parallel (left) and perpendicular (right) to the material flow and were created in two different structure heights (top/bottom).

Subsequently, the tools were functionalized as described before leading to C18PA-monolayers chemically attached by P-O-M bonds and distal alkyl-chains (SAM) [57]. Afterwards the specimens were tested in the tribometer and the adhered aluminum volume was measured via WLI. Figure 5.2 depicts the measured torque

curves while Fig. 5.3 shows the results of the WLI measurements (contour plot as well as overall adhered aluminum volume).

Independently of the pattern, non-functionalized structuring heights of 10 µm lead to large aluminum adhesion accumulating on the surface features. Tool surfaces structured similarly but functionalized showed a reduction in transferred torque and in aluminum adhesion especially with measured reductions of more than 90 % [62]. Non-functionalized surfaces with structuring heights of 1 µm lead to a similar reduction in aluminum adhesion. However, no significant difference in aluminum adhesion was determined between functionalized and non-functionalized star-shaped surfaces with 1 µm structuring height. Contrarily, the functionalized surface with a 1 µm circular pattern showed the smallest amount of aluminum adhesion for all structured surfaces, which was determined 75 % lower compared to the non-functionalized structured reference. Compared to both, non-functionalized structured or flat polished references as well as to the polished and functionalized tool surface, the 1 µm circular structured and functionalized tool revealed a continuous transferred torque during testing which was observed 2-fold lower compared to the structured non-functionalized reference as well as the functionalized polished reference.

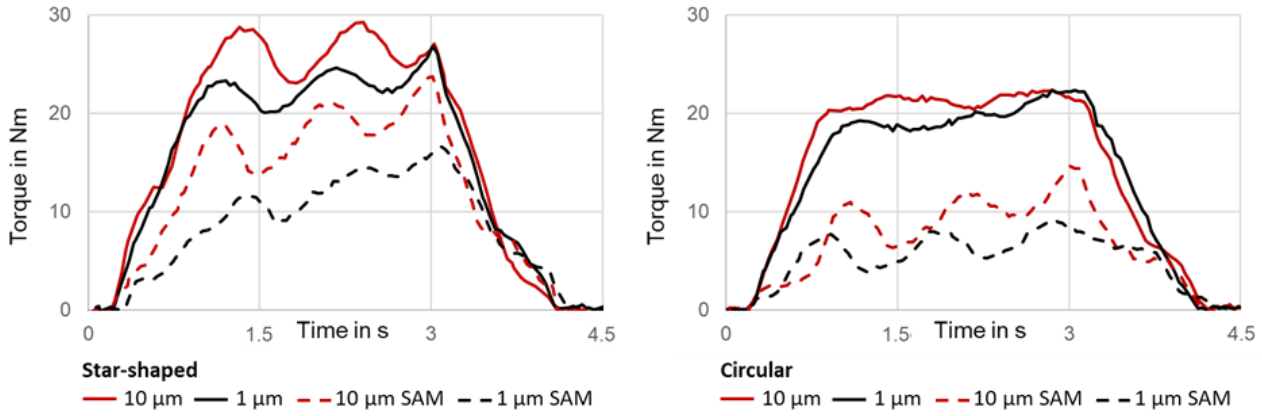

Fig. 5.2: Torque curves for star-shaped and circular structures with different structure heights and functionalization. Lower torque indicates less friction [62]

Although reduced, high resolution secondary electron microscopy disclosed the aluminum adhesion on functionalized 1 µm star-shaped and circular patterned tools (Figure 5.4). Here, a distinct difference in aluminum adhesion was observed for the two different structures: While the adhesion generally occurs on the substructures of the laser structured surfaces originating from the laser displacement, larger volumes of aluminum were discovered for the star-shaped structure compared to the circular structure. For the latter, the aluminum adhesion is very thin, assumable less than 1 µm in thickness, so that the structure underneath the adhesion is still visible when detecting back-scatter electrons. The micrograph (Figure 5.4f) exposes an experimentally found on-set of aluminum adhesion on micro-rough surface features of martensite needles and dendrites stemming from the laser structuring process involving remelting of the surface. It is assumed that the aluminum adhesion occurs first on these structures due to their roughness and exposition in the surface [62].

Based on this result, the possibility of smoothing the martensitic structure by laser processing was investigated. Laser micro polishing was used because it creates very shallow melt pools of only a few micrometer depth. This leads to higher cooling rates compared to laser macro polishing with cw laser radiation. Therefore the material solidifies very rapidly and homogeneously, theoretically giving it less time to form martensite. The process parameters were a beam diameter d_L of 250 µm, pulse durations t_P of 1 µs, repetition frequency f_{rep} of 20 kHz, scanning velocity v_S of 500 mm/s, track offset d_y of 30 µm. Average laser power P_L was varied to achieve different degrees of remelting. The result is that this process is able to gradually smoothen the micro structure of the martensite needles from a partial remelting with lower laser power (65 W) to a complete remelting with higher laser power (80 W) (See Fig 5.5). The mechanisms leading to the smoothing of the martensite structure must be further investigated by hardness measurements (nanoindenter) and high-resolution microstructure analysis.

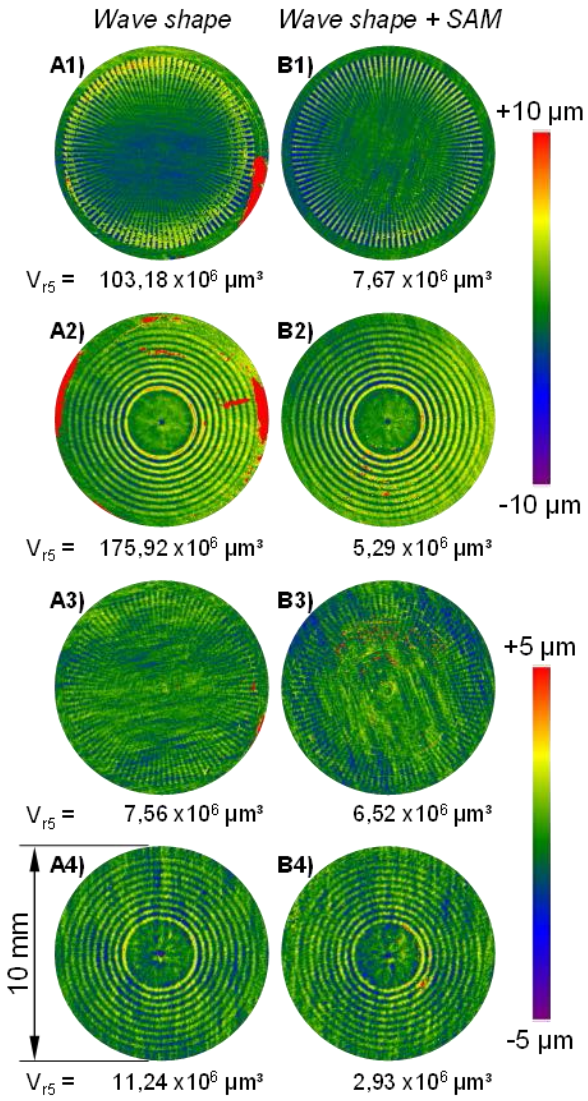

Fig. 5.3: WLI measurements of the overall adhered Al volume of different surfaces after testing in the tribometer. Columns: A) structured (Wave shape); B) structured and functionalized; Rows: 1) deep star-shaped structure (10 µm); 2) deep circular structure (10 µm); 3) smooth star-shaped structure (1 µm); 4) smooth circular structure (1 µm). [62]

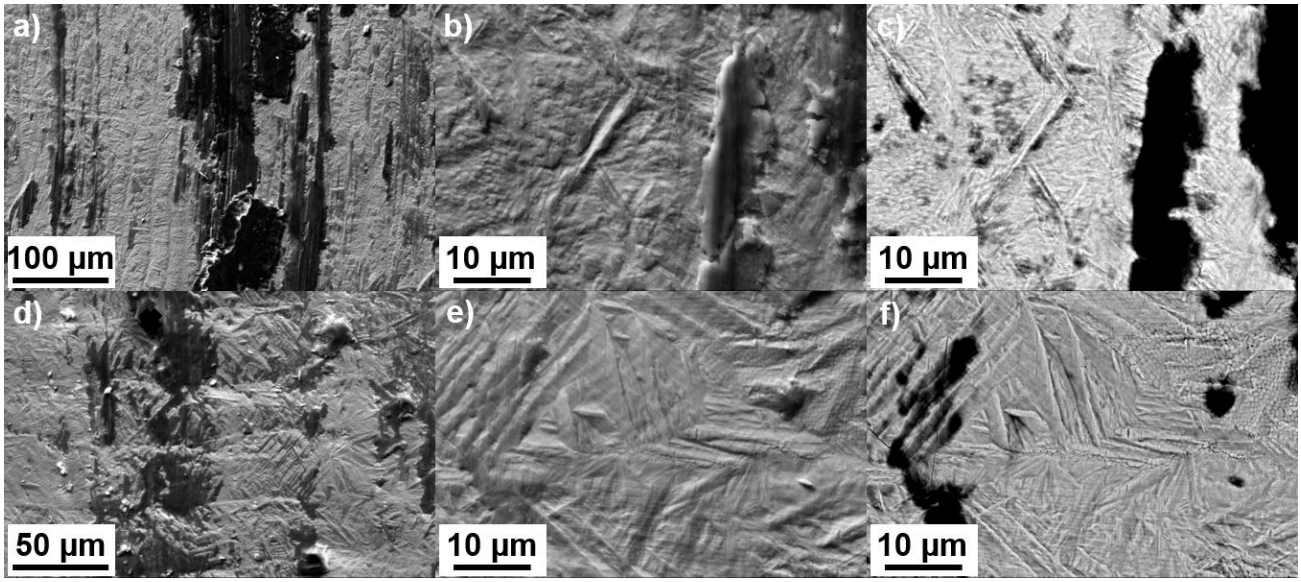

Fig. 5.4: Scanning electron micrographs of aluminum adhesion (dark) detected on 1 µm laser structured and functionalized surfaces with star-shape (first row) and circular structure (second row). High resolution secondary electron micrographs (b and e) of overviews (a and d) and back-scatter electron micrographs of the same area expose substructures, e.g. martensite needles and dendrites, as onset of aluminum adhesion. [62].

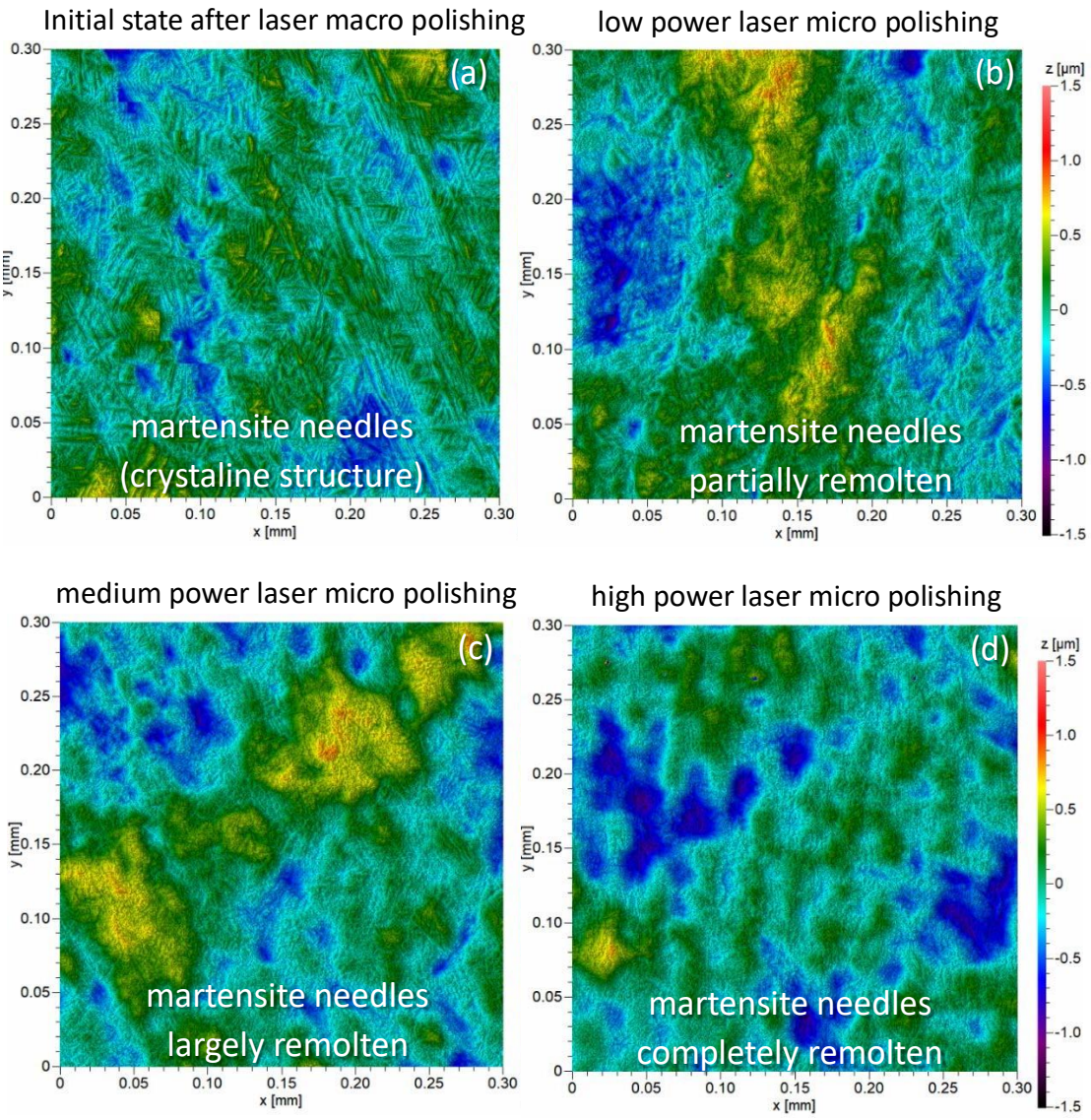

Fig. 5.5: False color representation of WLI measurements on tribometer sample surfaces (material: 1.2343 ESR). After macro laser polishing (a) the sharp crystalline martensite needles are clearly visible. With increasing laser power the laser micro polishing process with its short lived shallow melt pools is able to gradually remelt these micro structures either partially (b) or completely (d).

6 Conclusion and future work

Despite many possible savings potentials, dry bulk metal forming is currently hardly used in an industrial environment. The reason for this is the intensive mechanical and chemical interaction between the surfaces of the workpiece and the tool without the use of separating lubricants. The increased risk of adhesion and abrasion is associated with a poorer surface quality of the produced workpieces as well as a shorter tool life or in the worst case immediate failure of the tools. The core challenge therefore lies in reducing the interaction in the effective joint between workpiece and tool by other means in order to achieve comparable friction and wear characteristics as in the lubricated process. In order to accomplish this task, novel technical surfaces on tools and a reduction of the tribological loads, if necessary also by accepting a reduction of the process window can be considered.

The reported project has addressed this challenge and provided insights in various areas. These include:

- The development of a tribological test sequence for the full forward extrusion of aluminum
- The analysis of the process challenges and existing control variables in the implementation of dry impact extrusion

- The development of novel surface modifications using laser remelt processing for different materials and more complex geometries
- The understanding of adhesion formation on atomic level
- The development of a novel functionalization concept with self-assembling monolayers (SAM)
- The characterization of the basic suitability of a combination of laser processing and functionalization for the dry forming of aluminum

The combination of laser processing and functionalization with self-assembling monolayers offers great potential and first test results in the tribological test sequence show the basic functionality by means of a reduced interaction of the tool edge layer with aluminum. Especially the tests in the tribometer prove the performance capability, which have to be confirmed within further research work. This must be accompanied by a deeper understanding of the combined surface modification.

In the future, the connection of the self-assembling monolayers to the die must be further optimized so that a longer service life can be achieved. Besides enhancing the surface functionalization itself, a tribological active coating, e.g. refractory metal sulfides, applied in between self-assembling monolayer and die surface may further preserve the structural integrity of the protective surface architecture and obstruct detrimental asperity contacts. Simultaneously, low interaction is maintained by small van-der-Waals interaction between self-assembling monolayer and reactive aluminum. Laser processing of the tool surfaces not only changes the tool topography by polishing or structuring, but can also achieve a chemical optimization of the surface layer by breaking up carbides, which are considered critical for functionalization. Thus, more homogeneous surfaces could be created for the connection of the SAM. Combining laser surface modification techniques and protective surface coating and functionalization enclosed in one set-up may constitute an experiment with large impact on industrial tool manufacturing beyond dry metal forming applications.

The vision of dry bulk metal forming of aluminum has not yet been fully achieved for the process example shown. The tools for effective testing of the surface modifications are now available, so that further and targeted research into dry forming can be carried out in the future. Future research work and investigations must show within which process- and material-related limits dry extrusion of aluminum is economically feasible.

Acknowledgement

The authors gratefully acknowledge the financial support of the Deutsche Forschungsgemeinschaft (DFG) within the priority programme SPP 1676 “Dry Metal Forming” (project number: 244932637). Moreover, the authors would like to thank all colleagues and students at the various institutes who have contributed to this project over the past six years.

References

[1] G. Spur,H. Hoffmann,R. Neugebauer, "Handbuch Umformen. Handbuch der Fertigungstechnik“: Hanser Verlag. München, 2012.
[2] S. Wagener, 1996, "3D-Beschreibung der Oberflächenstrukturen von Feinblechen“. Dissertation. Stuttgart, Universität Stuttgart.
[3] Z. M. Hu, T. A. Dean, "A study of surface topography, friction and lubricants in metalforming.” International Journal of Machine Tools and Manufacture, 40, S. 1637–1649, 2000.
[4] K. Lange, L. Cser, M. Geiger, J. A. G. Kals, "Tool Life and Tool Quality in Bulk Metal Forming.” CIRP Annals - Manufacturing Technology,
41 (2), S. 667–675, 1992.
[5] S. Kalpakjian,S. R. Schmid,E. Werner, "Werkstofftechnik.“ 5. Auflage: Pearson Studium. München, 2009.
[6] H. Czichos,K.-H. Habig,E. Santner,M. Woydt,K. Gerschwiler, "Tribologie-Handbuch: Reibung und Verschleiß“: Vieweg. Wiesbaden, 2003. [7] A. Elsen, P. Groche, "Adhesive Wear in Dry Sliding of Aluminum.” In: A. S. Khan (Hg.): Proceedings of the 16th International Symposium
on Plasticity and its Current Applications. Detroit, Mich., January 3 - 8, 2010. Fulton, Md.: NEAT Press, 2010.
[8] J. An, Y. B. Liu, Y. Lu, Q. Y. Zhang, C. Dong, "Dry sliding wear behavior of hot extruded Al–Si–Pb alloys in the temperature range 25– 200 °C.” Wear, 256 (3-4), S. 374–385, 2004.
[9] N. Bay, "The state of the art in cold forging lubrication.” JMPT, 46, S. 19–40, 1994.
[10] Y. Liu, A. Erdemir, E. I. Meletis, "A study of the wear mechanism of diamond-like carbon films.” Surface and Coatings Technology, 82, S.
48–56, 1996.
[11] N. Bay, A. Azushima, P. Groche, I. Ishibashi, M. Merklein, M. Morishita et al., "Environmentally benign tribo-systems for metal forming.” CIRP Annals - Manufacturing Technology, 59 (2), S. 760–780, 2010.
[12] R. Farrell, E. Horner, "Metal Cleaning.” Metal Finishing, S. 86–97, 2007.
[13] A. Felde, A. Schwager, "Einsatz von Keramikmatrizen für das Kalt- und Halbwarm- Vollvorwärts-Fließpressen.“ Schmiede-Journal, S. 14– 15, 2005.
[14] F. Clarysse, W. Lauwerens, M. Vermeulen, "Tribological properties of PVD tool coatings in forming operations of steel sheet.” Wear, 264 (5-6), S. 400–404, 2008.
[15] W. Tillmann, E. Vogli, J. Herper, M. Haase, "Nanostructured Bionic PVD-Coatings for Forming Tools.” KEM, 438, S. 41–48, 2010.

[16] F. Rovere, D. Music, J. M. Schneider, P. H. Mayrhofer, "Experimental and computational study on the effect of yttrium on the phase stability of sputtered Cr–Al–Y–N hard coatings." Acta Materialia, 58 (7), S. 2708–2715, 2010.
[17] F. Rovere, D. Music, S. Ershov, M. Baben, H.-G. Fuss, P. H. Mayrhofer, J. M. Schneider, "Experimental and computational study on the phase stability of Al-containing cubic transition metal nitrides." Journal of Physics D, 43 (3), S. 1–11, 2010.
[18] B. Kappes, 2005, "Über den Nachweis tribologischer Effekte mit Hilfe von Modellversuchen im Bereich der umweltfreundlichen Kaltmas-
sivumformung." Dissertation. TU Darmstadt, Darmstadt.
[19] A. Gåård, R. M. Sarih, 2012, "Influence of Tool Material and Surface Roughness on Galling Resistance in Sliding Against Austenitic Stainless Steel" (2). Online verfügbar unter http://download.springer.com/static/pdf/798/art%253A10.1007%252Fs11249-012-9934- 7.pdf?auth66=1364474884_70e7081fc4e4964ba748c1dbd8288f3b&ext=.pdf, zuletzt geprüft am 13.03.2013.
[20] W. Wilson, S. Kalpakjian, "Low-Speed Mixed Lubrication of Metal-Forming Processes." CIRP Annals Manufacturing Technology, 44 (1), S. 205–208, 1995.
[21] G. Ngaile, M. Gariety, T. Altan, "Enhancing Tribological Conditions in Tube Hydroforming by using Textured Tubes". Transactions of the ASME, 128, S. 674–676, 2006.
[22] M. Vermeulen, J. Scheers, "Micro-hydrodynamic effects in EBT textured steel sheet." International Journal of Machine Tools and Manu-
facture, 41, S. 1941–1951, 2001.
[23] K. Wagner, A. Putz, U. Engel, "Improvement of tool life in cold forging by locally optimized surfaces." JMPT, 177 (1-3), S. 206–209, 2006. [24] A. Gåård, P. Krakhmalev, J. Bergström, "Influence of tool steel microstructure on origin of galling initiation and wear mechanisms under
dry sliding against a carbon steel sheet." Wear, 267 (1-4), S. 387–393, 2009.
[25] P. Groche, B. Kappes, 2004, "Tribologie der Massivumformung - Modellprüfstände der Tribologie." Kapitel 1. In: W. J. Bartz (Hg.): Hand- buch der Tribologie und Schmierungstechnik: Expert Verlag (Tribologie und Schmierung bei der Massivumformung, 13), S. 1–14.
[26] P. Groche, J. Filzek, G. Nitzsche, "Local Contact Conditions in Sheet Metal Forming and Their Simulation in Laboratory Test Methods." Production Engineering, 11 (1), S. 55–60, 2004.
[27] M. Burgdorf, "Über die Ermittlung des Reibwertes für Verfahren der Massivumformung durch den Ringstauchversuch." Werkzeugmaschi-
nen und Fertigungstechnik. Teil II: Umformtechnik. Industrie- Anzeiger, 89 (5), S. 15–20, 1967.
[28] D. Hemyari, 1999, "Methode zur Ermittlung von Konstitutivmodellen für Reibvorgänge in der Massivumformung bei erhöhten Temperatu- ren." Berichte aus Produktion und Umformtechnik (Band 43). Dissertation. TU Darmstadt, Darmstadt.
[29] C. Karadogan, R. Grueebler, P. Hora, "A New Cone-Friction Test for Evaluating Friction Phenomena in Extrusion Processes." KEM, 424, S. 161–166, 2009.
[30] P. Hora, M. Gorji, B. Berisha, "Modeling of Friction Phenomena in Extrusion Processes by Using a New Torsion-Friction Test." KEM, 491,
S. 129–135, 2011.
[31] M. Geiger, T. Herlan, Fließpressen: Kapitel 3.5.1, in: G. Spur, H. Hoffmann, R. Neugebauer (Ed.), Handbuch Umformen: Handbuch der Fertigungstechnik, Hanser Verlag, München, 2012, S. 318-387.
[32] M. Teller, „Tribologische Prüfkette zur Analyse trockener Umformprozesse am Beispiel des Vollvorwärtsfließpressens von Aluminium", Dissertation, Verlag Mainz, Aachen, 2019.
[33] N. Bay, ICFG (International Forging Group): Objectives History Published documents, International Cold Forging Group, 1992, S. 48-50,
78-82.
[34] M. Teller, I. Ross, A. Temmler, R. Poprawe, S. Prünte, J.M. Schneider, G. Hirt, "Investigation of Friction Conditions in Dry Metal Forming of Aluminum by Extended Conical Tube-Upsetting Tests", Key Engineering Materials 767, S. 189-195, 2018.
[35] M. Teller, S. Seuren, M. Bambach, G. Hirt, "A New Compression-Torsion-Tribometer with Scalable Contact Pressure for Characterization of Tool Wear during Plastic Deformation," Conference Papers in Science, Article ID 496515, 2015, doi:10.1155/2015/496515.
[36] M. Teller, M. Bambach, G. Hirt, "A compression-torsion-wear test achieving contact pressures of up to eight times the initial flow stress of
soft aluminium ", CIRP Annals 64, Vol. 1, 2015, doi:10.1016/j.cirp.2015.04.086.
[37] M. Teller, G. Hirt, I. Ross, M. Küpper, A. Temmler, R. Poprawe, S. Prünte, "Einfluss des Handpolierens von Probenkörpern auf Gestaltab- weichungen erster Ordnung und das Verschleißverhalten in Tribometerversuchen", Dry Metal Forming Open Access Journal FMT 4, S. 31-34, 2018.
[38] M. Teller, M. Bambach, G. Hirt, I. Ross, A. Temmler, R. Poprawe, H. Bolvardi, S. Prünte, J. M. Schneider, "Investigation of the suitability of surface treatments for dry cold extrusion by process-oriented tribological testing", Key Engineering Materials 651-653, S. 473-479, 2015.
[39] M. Teller, G. Hirt, „Trockene Tribosystems prozessnah beschreiben", MM Maschinenmarkt 45, 2015, S. 36-38.
[40] M. Teller, G. Hirt, I. Ross, A. Temmler, R. Poprawe, S. Prünte, J.M. Schneider, "Konzept zur Bearbeitung und tribologischen Prüfung von Fließpressmatrizen für das Trockenumformen von Aluminium", Dry Metal Forming Open Access Journal FMT 3, S. 73-80, 2017.
[41] E. Willenborg, „Polieren von Werkzeugstählen mit Laserstrahlung", Dissertation, Shaker Verlag, Aachen, 2005. [42] A. Temmler, „Laserumschmelzstrukturierung", Dissertation, Shaker Verlag, Aachen, 2012.
[43] I. Ross, A. Temmler, R. Poprawe, M. Teller, G. Hirt, S. Prünte, "Untersuchung zur Oberflächenmodifikation mittels Laserpolieren für das schmiermittelfreie Kaltfließpressen von Aluminium", Dry Metal Forming Open Access Journal FMT 1, S. 143-151, 2015.
[44] A. Temmler, I. Roß, M. Cortina, R. Poprawe, "Oberflächenfunktionalisierung des Werkstoffs 1.2379+ mittels Randschichtumschmelzen mit Laserstrahlung zur Entwicklung von angepassten Oberflächentopographien für das schmiermittelfreie Kaltfließpressen von Alumi- nium", Dry Metal Forming Open Access Journal FMT 3, S. 62-72, 2017.
[45] A. Temmler, M. Comiotto, I. Roß, M. Kuepper, D. M. Liu, R. Poprawe, „Surface structuring by laser remelting of 1.2379 (D2) for cold forging tools in automotive applications", J. Laser Appl. 31, 022017, doi: 10.2351/1.5070077, 2019.
[46] I. Ross, A. Temmler, M. Küpper, S. Prünte, M. Teller, J.M. Schneider, R. Poprawe, "Laser Polishing of Cold Work Steel AISI D2 for Dry Metal Forming Tools: Surface Homogenization, Refinement and Preparation for Self-Assembled Monolayers", Key Engineering Materials 767, S. 69-76, 2018.
[47] M. Teller, S. Prünte, I. Ross, A. Temmler, J.M. Schneider, G. Hirt, "Tribological investigations of the applicability of surface functionalization
for dry extrusion processes", AIP Conference Proceedings 1896, S. 140001, 2017, doi: 10.1063/1.5008157.
[48] J. Emmerlich, D. Music M. Braun, P. Fayek, F. Munnik, J.M. Schneider, "A proposal for an unusually stiff and moderately ductile hard coating material: Mo2BC", Journal of Physics D: Applied Physics 42 (18), S. 185406, 2009, doi: 10.1088/0022-3727/42/18/185406.
[49] H. Bolvardi, J. Emmerlich, S. Mráz, M. Arndt, H. Rudigier, J.M. Schneider, "Low temperature synthesis of Mo2BC thin films", Journal of Applied Mechanics 542, S. 5–7, 2013, doi: 10.1016/j.tsf.2013.07.021.
[50] S. Djaziri, S. Gleich, H. Bolvardi, C. Kirchlechner, M. Hans, C. Scheu et al., "Are Mo2BC nanocrystalline coatings damage

resistant?
Insights from comparative tension experiments", Surface and Coating Technology 289, S. 213–218, 2016, doi: 10.1016/j.surf- coat.2016.02.010.
[51] H. Bolvardi, D. Music, J.M. Schneider, "Atomic scale onset of Al adhesion on Mo2BC", Thin Solid Films 589, S. 707–711, 2015, doi: 10.1016/j.tsf.2015.06.057.
[52] H. Bolvardi, D. Music, J.M. Schneider, "Interaction of Al with O2 exposed Mo2BC", Applied Surface Science 332, S. 699–703, 2015, doi: 10.1016/j.apsusc.2015.01.237.
[53] D. Godfrey, Boundary Lubrication, in: P.M. Ku (Ed.), Interdisciplinary approach to friction and wear, GPO, United States, 1968
[54] J.C. Love, L.A. Estroff, J.K. Kriebel, R.G. Nuzzo, G.M. Whitesides, "Self-assembled monolayers of thiolates on metals as a form of nano- technology", Chemical Reviews 105, S. 1103–1169, 2005, doi: 10.1021/cr0300789.
[55] G. Guerrero, J.G. Alauzun, M. Granier, D. Laurencin, P.H. Mutin, "Phosphonate coupling molecules for the control of surface/ interface properties and the synthesis of nanomaterials", Dalton Transactions 42 (35), S. 12569–12585, 2013, doi: 10.1039/c3dt51193f.
[56] X. Xiao, J. Hu, D.H. Charych, M. Salmeron, "Chain Length Dependence of the Frictional Properties of Alkylsilane Molecules Self-Assem-
bled on Mica Studied by Atomic Force Microscopy", Langmuir 12 (2), S. 235–237, 1996, doi: 10.1021/la950771u.
[57] S. Prünte, D. Music, J.M. Schneider, M. Teller, G. Hirt, P.H. Mutin, G. Ramanath, "Decreasing friction during Al cold forming using a nanomolecular layer", Journal of Vacuum Science & Technology A 35 (2), S. 20605, 2017, doi: 10.1116/1.4972515.
[58] A. Khassanov, H.-G. Steinrück, T. Schmaltz, A. Magerl, M. Halik, "Structural investigations of self-assembled monolayers for organic electronics: results from X-ray reflectivity", Accounts of Chemical Research 48 (7), S. 1901–1908, 2015, doi: 10.1021/acs.ac-counts.5b00022.
[59] S. Prünte, D. Music, V.L. Terziyska, C. Mitterer, J.M. Schneider, "Molecular Coverage Determines Sliding Wear Behavior of n-Octade- cylphosphonic Acid Functionalized Cu–O Coated Steel Disks against Aluminum", Materials 13 (2), S. 280, 2020, doi: 10.3390/ ma13020280.
[60] A. Raman, R. Quinones, L. Barriger, R. Eastman, A. Parsi, E.S. Gawalt, "Understanding organic film behavior on alloy and metal oxides", Langmuir 26 (3), S. 1747–1754, 2010, doi: 10.1021/la904120s.
[61] I. Ross, A. Temmler, E. Willenborg, R. Poprawe, M. Teller, “Investigation of the influence of laser surface modifications on the adhesive wear behavior in dry cold extrusion of aluminum“, Proceedings of Lasers in Manufacturing (LiM), 2015.
[62] M. Teller, I. Ross, S. Prünte, A. Temmler, M. Küpper, R. Poprawe et al., "Probing the potential of structured and surface functionalized tools for dry cold forging of aluminium", MATEC Web of Conferences 190, S. 14010, 2018, doi: 10.1051/ matecconf/201819014010.